Modeling and Simulation of a Complex Fluid: Wormlike Micellar Solutions

Michael Cromer, L. Pamela Cook

Department of Mathematical Sciences, University of Delaware

and

Gareth H. McKinley

Department of Mechanical Engineering, MIT

Mathematical and Computational Sciences Division Seminar
National Institute of Standards and Technology - Gaithersburg, MD
November 30, 2010

Supported by NSF-DMS-0807395 and NSF-DMS-0807330

Outline

- BACKGROUND
  - Properties of wormlike micellar solutions
  - Development of an elastic network (scission/reforming) model (VCM)

- 1D CHANNEL FLOW
  - Apparent slip boundary layer
  - Time dependent interior diffusive layer
  - Non-local effects

- NUMERICS
  - ADDS (Adaptive Domain Decomposition Spectral) Method

- CHANNEL FLOW - LINEAR STABILITY
  - Interfacial instability
  - Diffusive restabilization

- EXTENSIONAL FLOW
  - Rupture

Wormlike Micellar Solutions

Applications

- Oil industry (fracturing fluids, EOR)
- Household and cosmetic products
- Drag/friction reducers
- Biotechnology

Complex geometries and unsteady flows

Therefore it is important for us to fully understand the steady and transient rheology of these entangled microstructured solutions.

Wormlike Micellar Solutions

Surfactant Molecules

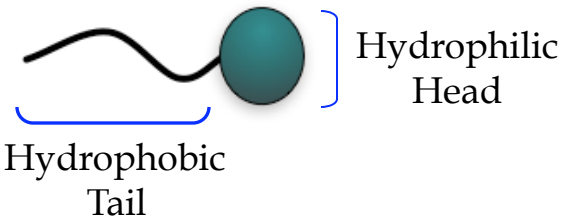

Critical Micellar Concentration

Self-assemble

Wormlike Micelles

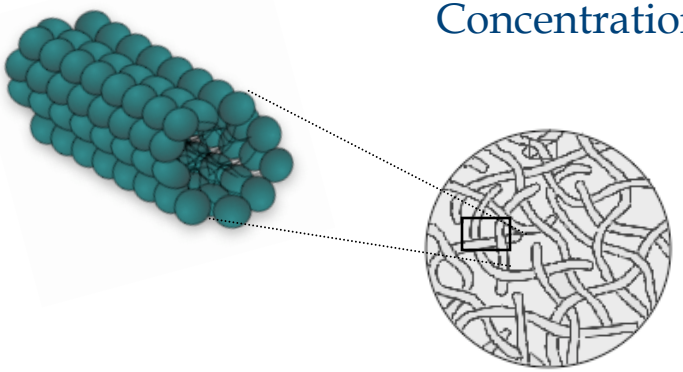

Overlap Concentration

Entangled Systems

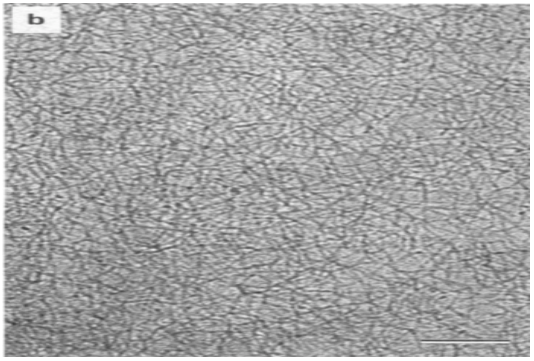

Clausen et al. (1992) J. Phys. Chem.

Different properties depend on surfactant and salt concentration†

- CPyCl/NaSal
- CTAB/NaSal
- EHAC/NaSal
- TTABr/NaSal

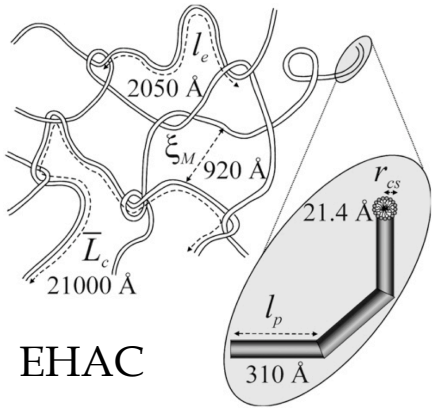

EHAC

Schubert et al. (2003) Langmuir

†*Disclaimer: all wormlike micellar solutions are not created equal!*

UCM (upper convected Maxwell) Model

$$\lambda \boldsymbol{\tau}_{(1)} + \boldsymbol{\tau} = \eta_0 \dot{\boldsymbol{\gamma}}$$

$$\boldsymbol{\tau} = \begin{pmatrix} \tau_{11} & \tau_{12} & \tau_{13} \\ \tau_{21} & \tau_{22} & \tau_{23} \\ \tau_{31} & \tau_{32} & \tau_{33} \end{pmatrix}$$

$$\dot{\boldsymbol{\gamma}} = \nabla \mathbf{v} + (\nabla \mathbf{v})^T$$

Upper convected time derivative:

$$(\cdot)_{(1)} = \frac{\partial (\cdot)}{\partial t} + (\mathbf{v} \cdot \nabla)(\cdot) - (\nabla \mathbf{v})^T \cdot (\cdot) - (\cdot) \cdot (\nabla \mathbf{v})$$

$$\mathbf{A} = \frac{\eta_0}{\lambda} \mathbf{I} - \boldsymbol{\tau}$$

Simple Shear: $\mathbf{v} = (v_1(x_2), 0, 0) = (\dot{\gamma}_{12}(t) x_2, 0, 0)$

$$\lambda(\tau_{12,t} - \dot{\gamma}_{12}\tau_{22}) + \tau_{12} = \eta_0 \dot{\gamma}_{12}$$

$$\lambda \tau_{22,t} + \tau_{22} = 0$$

$$\longrightarrow \quad \boxed{\lambda \tau_{12,t} + \tau_{12} = \eta_0 \dot{\gamma}_{12}}$$

UCM Model in SAOS

Small amplitude oscillatory shear (SAOS):

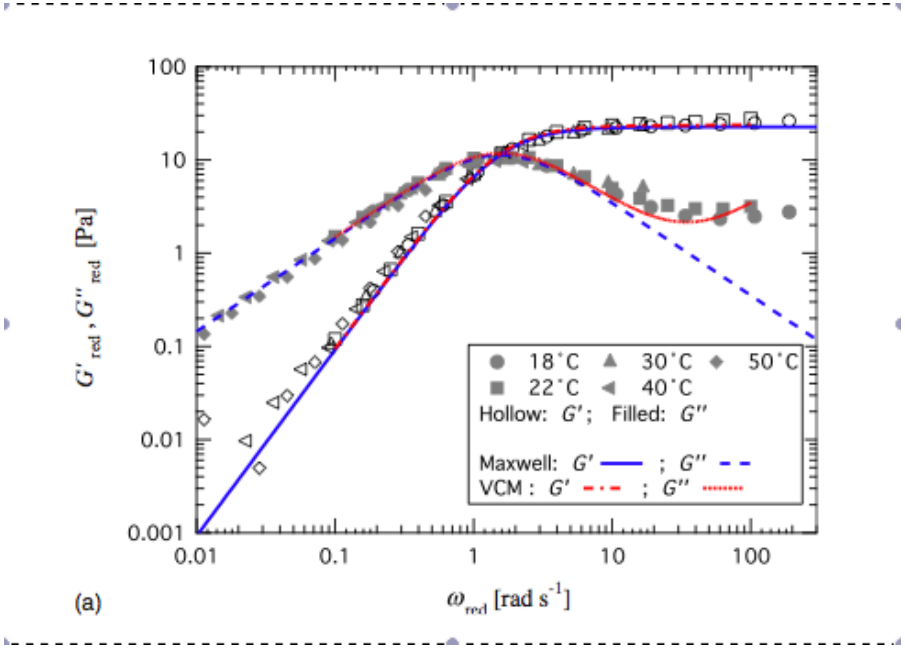

100/50 mM CPyCl/NaSal

$$\gamma_{12} = \gamma_0 \sin(\omega t) \quad \dot{\gamma}_{12} = \omega\gamma_0 \cos(\omega t)$$

$$\gamma_0 \ll 1$$

$$\tau_{12} = \gamma_0 \left[G' \sin(\omega t) + G'' \cos(\omega t)\right]$$

$$G' = G_0 \frac{(\lambda\omega')^2}{1+(\lambda\omega')^2} \quad G'' = G_0 \frac{\lambda\omega'}{1+(\lambda\omega')^2}$$

storage modulus, loss modulus

Relaxation time: $\lambda = 0.63$ s

Plateau modulus: $G_0 = \dfrac{\eta_0}{\lambda} = 22.6$ Pa

$$G'' = G' \Longrightarrow \lambda\omega = 1$$

Pipe et al, *J. Rheol.* (2010)

2nd Relaxation Time

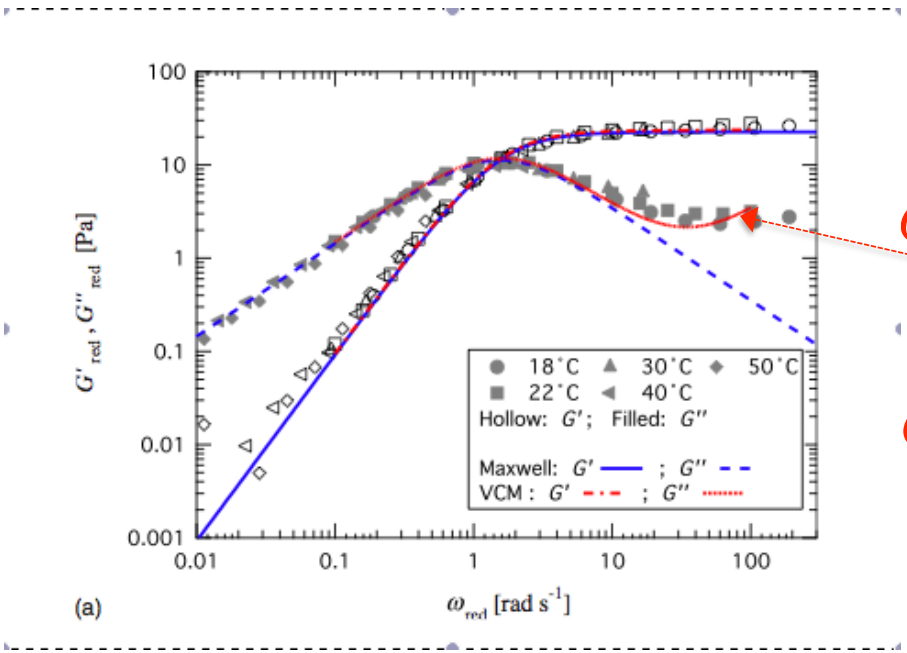

100/50 mM CPyCl/NaSal

BUT, for wormlike micelles, the storage and loss moduli are

$$G' = G_0 \left[\frac{(\lambda\omega')^2}{1+(\lambda\omega')^2} + n_2 \frac{(\lambda_2\omega')^2}{1+(\lambda_2\omega')^2} \right]$$

$$G'' = G_0 \left[\frac{\lambda\omega'}{1+(\lambda\omega')^2} + n_2 \frac{\lambda_2\omega'}{1+(\lambda_2\omega')^2} \right]$$

$$\lambda_2 \ll \lambda$$

$$\lambda = 0.63 \text{ s}$$

$$\lambda_2 = 0.0011 \text{ s}$$

Pipe et al, *J. Rheol.* (2010)

Banding in Steady Shear Flow
Wormlike Micelles

Shear rate control:

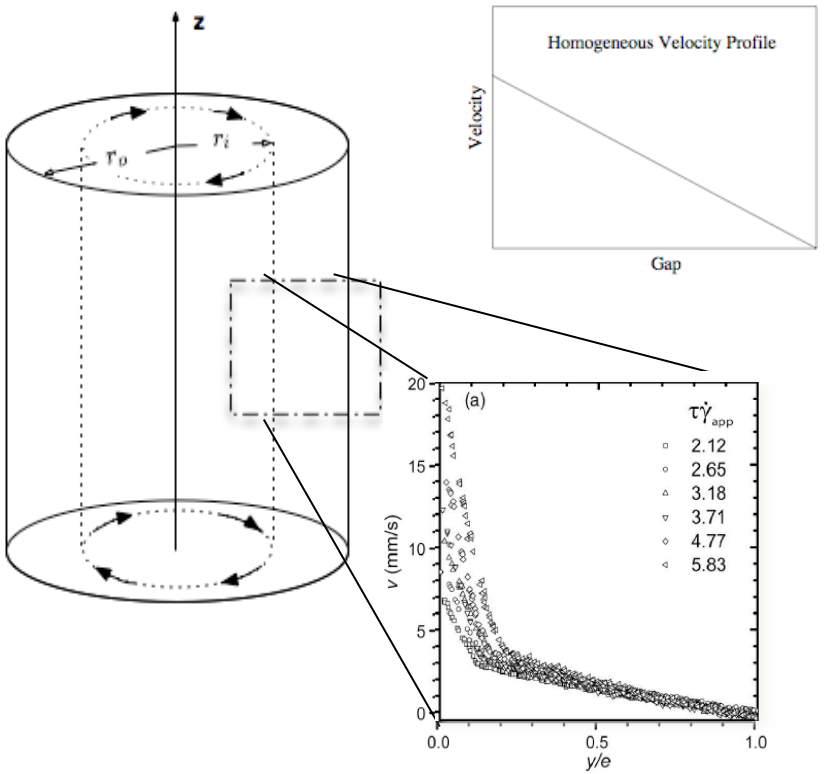

Hu and Lips, *J. Rheol.* (2005)

- Shear banding in the velocity profile for certain range of applied shear rates

- Plateau in the steady state flow curve

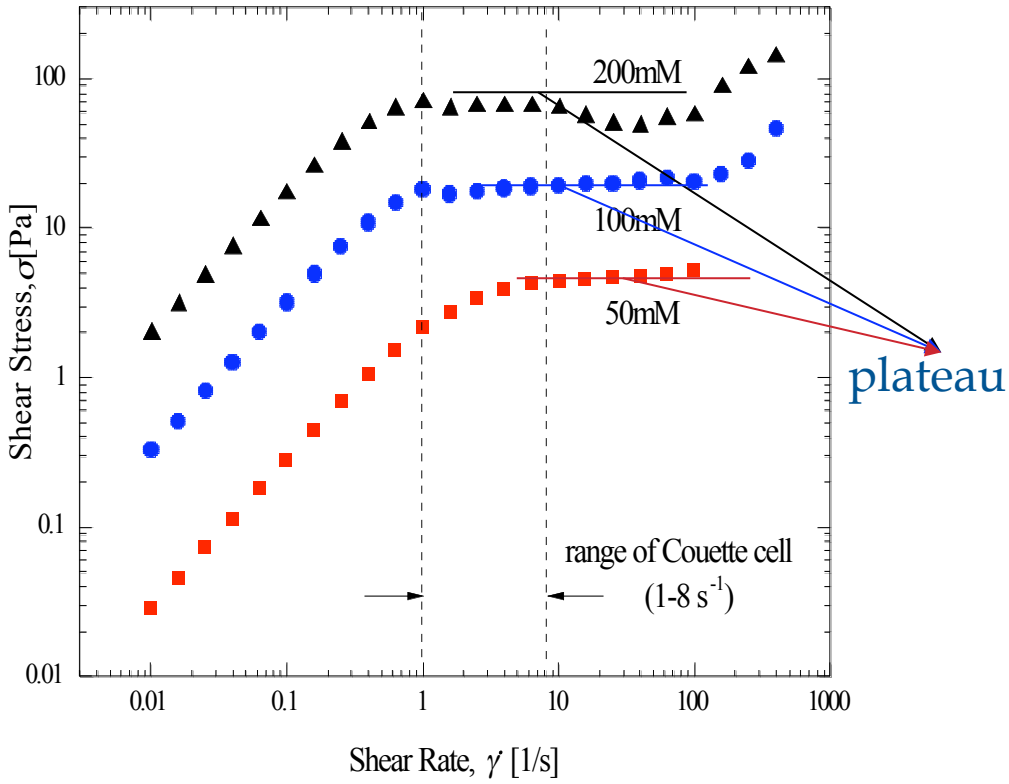

Miller and Rothstein, *JNNFM* (2007)

Banding in Steady Shear Flow
Constitutive Instability

Shear rate control:

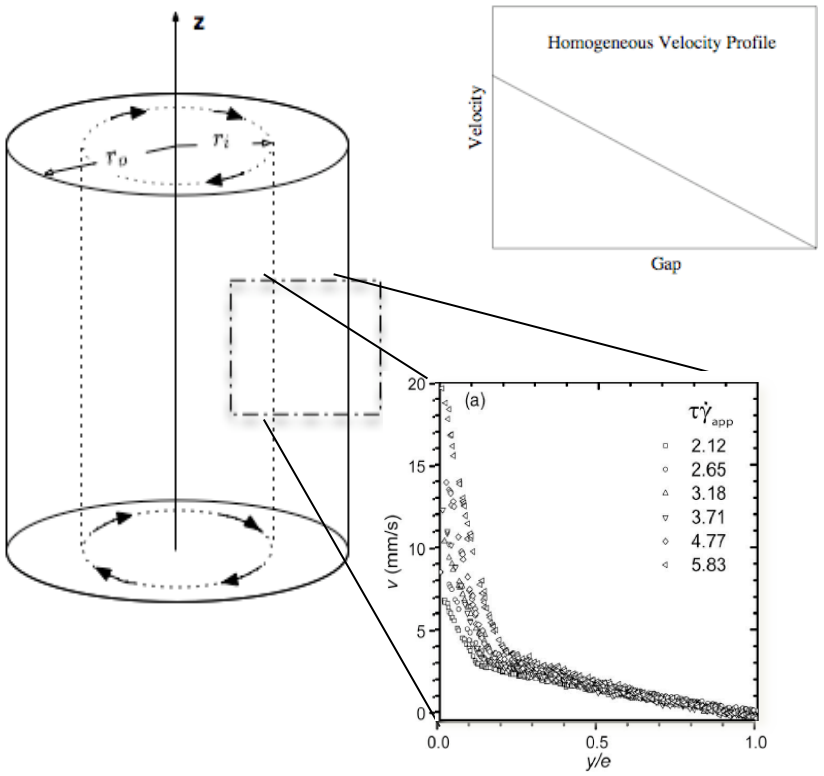

Hu and Lips, *J. Rheol.* (2005)

- Shear banding in the velocity profile for certain range of applied shear rates

- Non-monotone constitutive curve as a result of the breakage of the long chains.

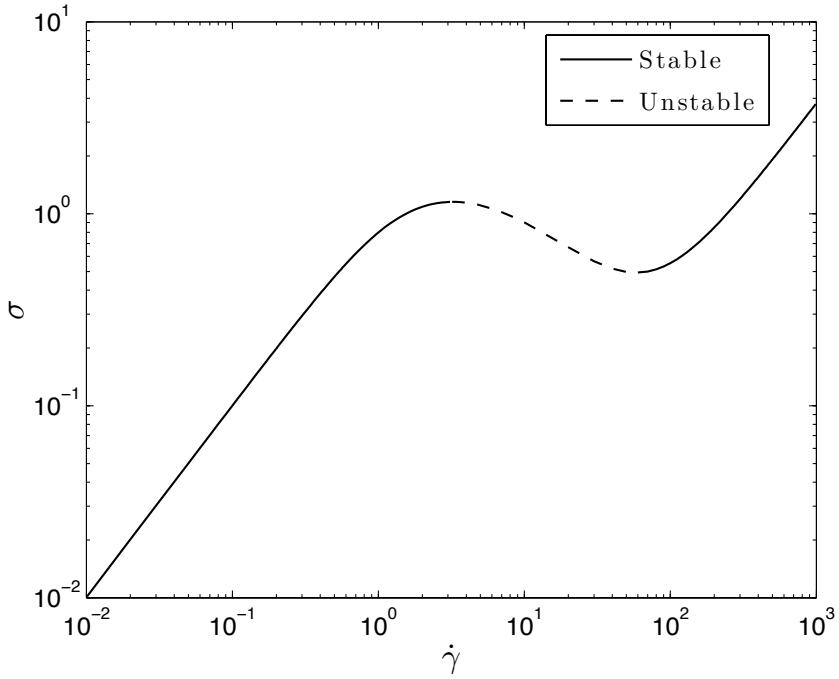

Banding in Steady Shear Flow
Constitutive Instability

Shear rate control:

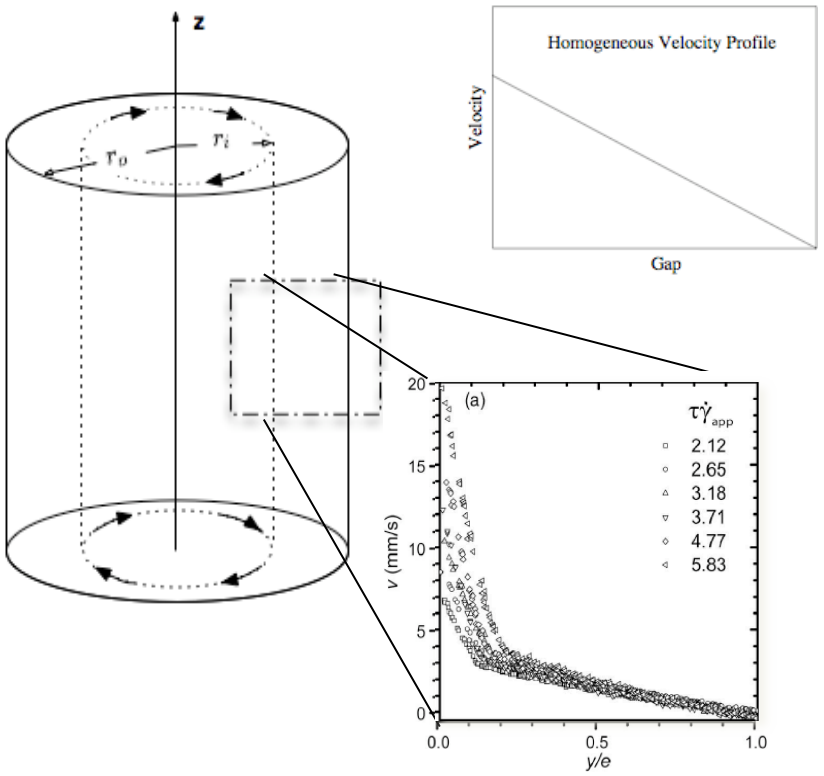

Hu and Lips, *J. Rheol.* (2005)

- Shear banding in the velocity profile for certain range of applied shear rates

- Given a shear rate within the unstable region, the model chooses shear rates on stable branch.

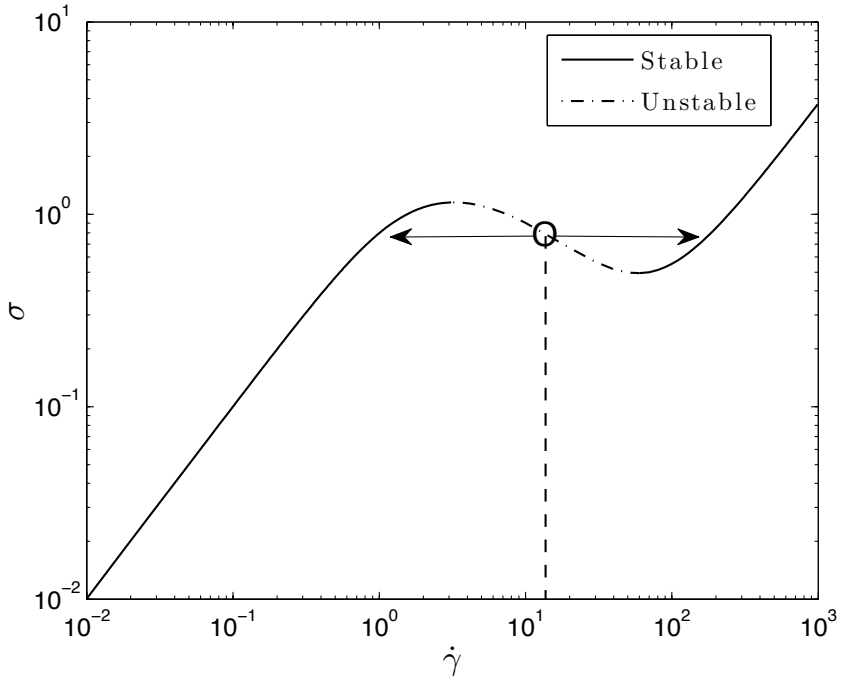

Banding in Steady Shear Flow
Constitutive Instability

Shear rate control:

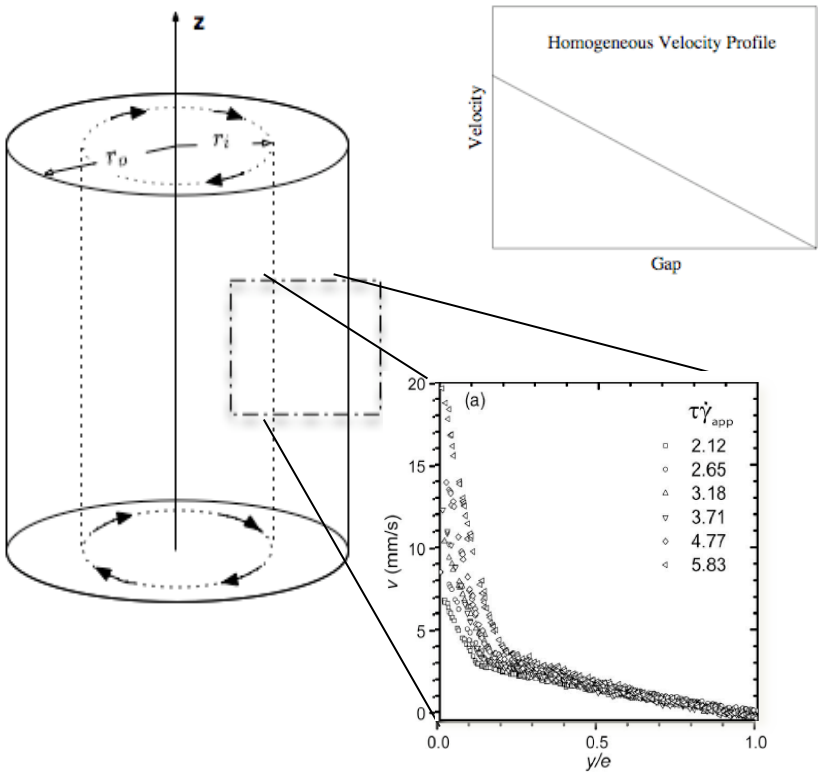

Hu and Lips, *J. Rheol.* (2005)

- Shear banding in the velocity profile for certain range of applied shear rates

- Because of this splitting, the flow becomes inhomogeneous and the stress plateau is observed corresponding to shear banding..

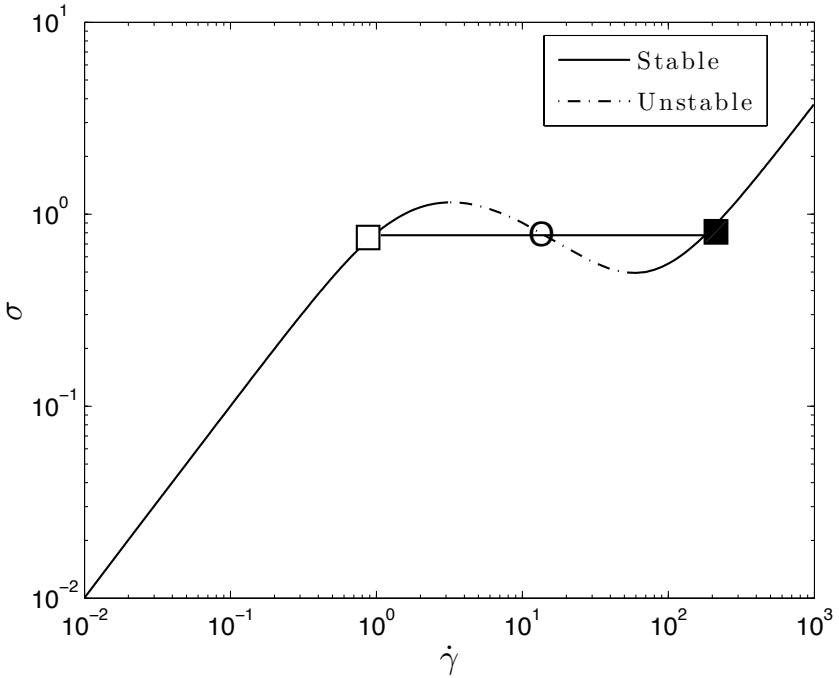

Nonlinear Single Species Models

Johnson-Segalman Model

$$\lambda \mathring{\mathbf{A}} + \mathbf{A} - G_0 \mathbf{I} = 0$$

Gordon-Schowalter derivative

$$\mathring{\mathbf{A}} = \mathbf{A}_{,t} + \mathbf{v} \cdot \nabla \mathbf{A} - \omega^T \cdot \mathbf{A} - \mathbf{A} \cdot \omega - \frac{a}{2} (\dot{\gamma} \cdot \mathbf{A} + \mathbf{A} \cdot \dot{\gamma})$$

Vorticity tensor

$$2\omega = \nabla \mathbf{v} - (\nabla \mathbf{v})^T$$

Giesekus Model

$$\lambda \mathbf{A}_{(1)} + \mathbf{A} - G_0 \mathbf{I} = -\alpha \frac{1}{G_0} (\mathbf{I} - \mathbf{A}) \cdot (\mathbf{I} - \mathbf{A})$$

Partially Extending Convected (PEC) Model

$$\lambda \mathbf{A}_{(1)} + \mathbf{A} - G_0 \mathbf{I} = -\frac{\xi}{3} \frac{\lambda}{G_0} (\dot{\gamma} : \mathbf{A}) \mathbf{A}$$

Ronald G. Larson, Constitutive Equations for Polymer Melts and Solutions, (© 1988)

Elastic Network Theory

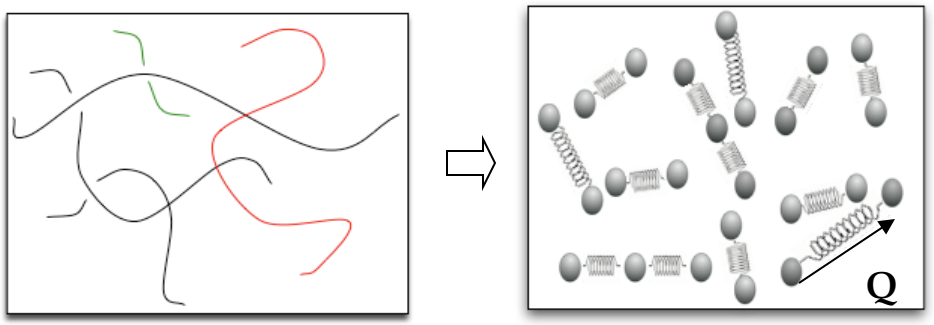

Micelles are modeled as breakable/ reformable elastic segments composed of Hookean springs connected to form a elastically active network.

$\Psi_\alpha(r, Q, t)\mathbf{dr}\,\mathbf{dQ}$: Number of segments in the range $\mathbf{dr}\,\mathbf{dQ}$ about $\mathbf{r},\mathbf{Q}$ at time t.

Evolution Equation – Network Theory

$$\frac{\partial \Psi_\alpha}{\partial t} = -\frac{\partial}{\partial \mathbf{r}} \cdot \left([\![\dot{\mathbf{r}}]\!] \Psi_\alpha \right) - \frac{\partial}{\partial \mathbf{Q}} \cdot \left([\![\dot{\mathbf{Q}}]\!] \Psi_\alpha \right) + \underline{\text{Breaking/Reforming}}$$

viscous drag + elastic resistance + Brownian motion

$[\![\cdot]\!]$ Average over momenta

Lodge, Yamamoto, Green; Bird et al. (1986)

Breaking and Reforming living polymers

Cates' theory (reptation/reaction):

Cates & Candau, *J.Phys.Cond. Matter 2* (1990)
Fielding & Cates, *Adv. In Phys.* (2006)

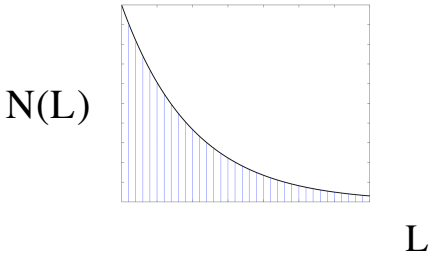

Assumptions:

- Length of each chain is a continuous variable L
- A chain can break with equal probability per unit time per unit length

Discrete breaking and reforming :

Assumptions:

- m species
- Discrete breakage points/lengths

Here we take m =2

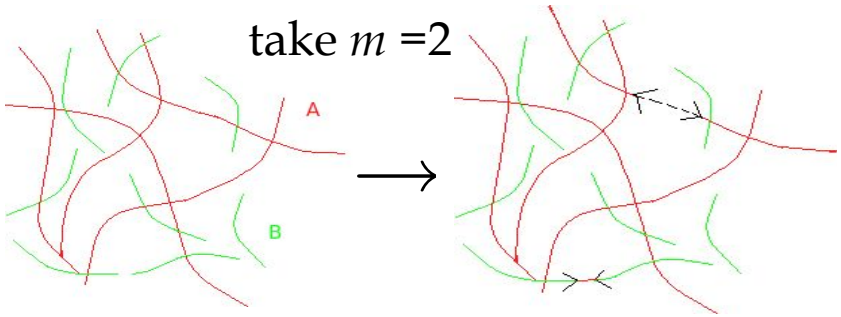

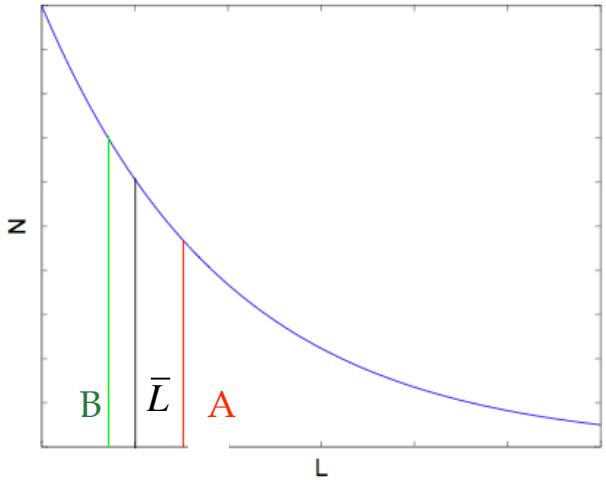

Long species A: $\Psi_A(r,Q,t)$ relaxation by reptation $\lambda_A \sim L^3 / L_E$

Short species B: $\Psi_B(r,Q,t)$ relaxation is Rouse-like $\lambda_B \sim (L/2)^2$

Governing Equations (VCM Model)

Number Densities:

$$n_\alpha(\mathbf{r},t) = \int \Psi_\alpha d\mathbf{Q}$$

$$\alpha = A,B$$

Configuration Tensors:

$$\mathbf{A} = \{\mathbf{QQ}\}_A = \int \mathbf{QQ}\Psi_A d\mathbf{Q}$$

$$\mathbf{B} = \{\mathbf{QQ}\}_B = \int \mathbf{QQ}\Psi_B d\mathbf{Q}$$

Constitutive equations

$$\mu \frac{Dn_A}{Dt} = 2\delta_A \nabla^2 n_A - \delta_A \nabla\nabla : \mathbf{A} + \tfrac{1}{2} c_B n_B^2 - c_A n_A$$

$$\mu \frac{Dn_B}{Dt} = 2\delta_B \nabla^2 n_B - 2\delta_B \nabla\nabla : \mathbf{B} - c_B n_B^2 + 2c_A n_A$$

$$\mu \mathbf{A}_{(1)} + \mathbf{A} - n_A \mathbf{I} = \delta_A \nabla^2 \mathbf{A} + c_B n_B \mathbf{B} - c_A \mathbf{A}$$

$$\epsilon \mu \mathbf{B}_{(1)} + \mathbf{B} - \tfrac{n_B}{2} \mathbf{I} = \epsilon \left[\delta_B \nabla^2 \mathbf{B} - 2c_B n_B \mathbf{B} + 2c_A \mathbf{A} \right]$$

Nonlinear fitting parameter

Breaking Rate:

$$c_A = \underbrace{\frac{\xi \mu}{3} \left(\dot{\gamma} : \frac{\mathbf{A}}{n_A} \right)}_{\text{Doi-Edwards/Larson}} + c_{Aeq}$$

Reforming Rate:

$$c_B = \text{constant} = c_{Beq}$$

Vasquez, Cook and McKinley, *JNNFM* (2007)

Governing Equations (VCM Model)

Number Densities:

$$n_\alpha(\mathbf{r},t) = \int \Psi_\alpha d\mathbf{Q}$$

$$\alpha = A,B$$

Configuration Tensors:

$$\mathbf{A} = \{\mathbf{QQ}\}_A = \int \mathbf{QQ}\Psi_A d\mathbf{Q}$$

$$\mathbf{B} = \{\mathbf{QQ}\}_B = \int \mathbf{QQ}\Psi_B d\mathbf{Q}$$

Constitutive equations

$$\mu\frac{Dn_A}{Dt} = 2\delta_A\nabla^2 n_A - \delta_A\nabla\nabla:\mathbf{A} + \tfrac{1}{2}c_B n_B^2 - c_A n_A$$

$$\mu\frac{Dn_B}{Dt} = 2\delta_B\nabla^2 n_B - 2\delta_B\nabla\nabla:\mathbf{B} - c_B n_B^2 + 2c_A n_A$$

$$\mu\mathbf{A}_{(1)} + \mathbf{A} - n_A\mathbf{I} = \delta_A\nabla^2\mathbf{A} + c_B n_B\mathbf{B} - c_A\mathbf{A}$$

$$\epsilon\mu\mathbf{B}_{(1)} + \mathbf{B} - \tfrac{n_B}{2}\mathbf{I} = \epsilon\left[\delta_B\nabla^2\mathbf{B} - 2c_B n_B\mathbf{B} + 2c_A\mathbf{A}\right]$$

Conservation of mass

$$\nabla\cdot\mathbf{v} = 0$$

Total Stress:

$$\boldsymbol{\Pi} = p\mathbf{I} + \underbrace{(n_A + n_B)\mathbf{I} - \mathbf{A} - 2\mathbf{B}}_{} - \beta\dot{\boldsymbol{\gamma}}$$

Conservation of momentum

$$E^{-1}\frac{D\mathbf{v}}{Dt} = -\nabla\cdot\boldsymbol{\Pi}$$

$$E^{-1} = \frac{\rho H^2}{\lambda_{eff}\eta_0}$$

Vasquez, Cook and McKinley, *JNNFM* (2007)

Governing Equations (VCM Model)

Number Densities:

$$n_\alpha(\mathbf{r},t) = \int \Psi_\alpha d\mathbf{Q}$$

$$\alpha = A,B$$

Configuration Tensors:

$$\mathbf{A} = \{\mathbf{QQ}\}_A = \int \mathbf{QQ}\Psi_A d\mathbf{Q}$$

$$\mathbf{B} = \{\mathbf{QQ}\}_B = \int \mathbf{QQ}\Psi_B d\mathbf{Q}$$

Constitutive equations

$$\mu\frac{Dn_A}{Dt} = 2\delta_A\nabla^2 n_A - \delta_A\nabla\nabla:\mathbf{A} + \tfrac{1}{2}c_B n_B^2 - c_A n_A$$

$$\mu\frac{Dn_B}{Dt} = 2\delta_B\nabla^2 n_B - 2\delta_B\nabla\nabla:\mathbf{B} - c_B n_B^2 + 2c_A n_A$$

$$\mu\mathbf{A}_{(1)} + \mathbf{A} - n_A\mathbf{I} = \delta_A\nabla^2\mathbf{A} + c_B n_B\mathbf{B} - c_A\mathbf{A}$$

$$\epsilon\mu\mathbf{B}_{(1)} + \mathbf{B} - \tfrac{n_B}{2}\mathbf{I} = \epsilon\left[\delta_B\nabla^2\mathbf{B} - 2c_B n_B\mathbf{B} + 2c_A\mathbf{A}\right]$$

Diffusion terms:

- Bhave et al., *J.Chem.Phys.* (1991)
- Beris and Mavrantzas, *J. Rheol.* (1994)

$$\delta_A = \frac{\lambda_A D_A}{H^2}$$

$$\delta_B = \frac{\lambda_B D_B}{H^2}$$

Stress boundary conditions:

- Dirichlet, Neumann or Mixed (Robin): (?)
  - Bhave et al., *J.Chem.Phys.* (1991), Mavrantzas et al., *J.Rheol.* (1992), Adams et al., *JNNFM* (2008), Black and Graham, *Macromolecules* (2001)

Parameters

Relaxation times:

λ_A	relaxation time of species A	$O(1)$ s
λ_B	relaxation time of species B	$O(10^{-4}) - O(10^{-3})$ s
λ_{eff}	effective relaxation time of the network	$O(10^{-1})$ s

$$\lambda_{eff} = \frac{\lambda_A}{1 + \lambda_A c'_{Aeq}}$$

$$\mu = \frac{\lambda_A}{\lambda_{eff}}$$

$$\epsilon = \frac{\lambda_B}{\lambda_A} = \frac{L_E}{4L} \ll 1$$

Viscosities:

η_s	dimensional solvent viscosity	$O(10^{-4})$ Pa s
η_0	dimensional zero shear rate micellar viscosity	$O(10)$ Pa s

$$\beta = \frac{\eta_s}{\eta_0} \ll 1$$

Geometric/fluid parameters

ρ	density of the solution	
H	length scale	μm $\rightarrow$ cm

$$E^{-1} = \frac{\rho H^2}{\lambda_{eff}\eta_0} \ll 1$$

Model parameters

δ_α	non-dimensional diffusion constants
ξ	flow-enhanced breakage rate

$$O(10^{-5}) \leq \delta_A = \frac{\lambda_A D_A}{H^2} \leq O(1)$$

Pressure-Driven Channel Flow

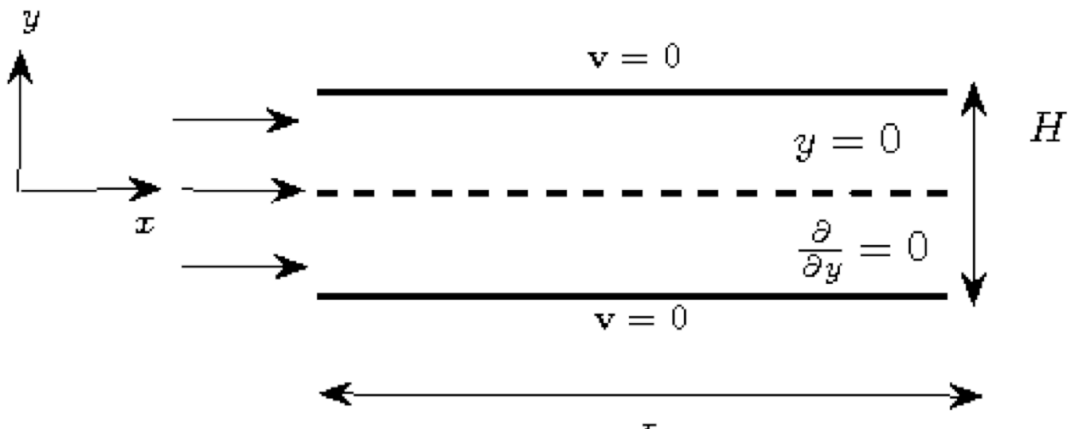

- Microfluidic devices can be used to explore non-local effects by systematically controlling the channel height, H.

$$\mathcal{P} = \frac{\Delta p H}{L G_0} \qquad \delta = \frac{\lambda_A D_A}{H^2} \quad O(10^{-11})\mathrm{m}^2/\mathrm{s} \leq D_A \leq O(10^{-9})\mathrm{m}^2/\mathrm{s}$$

- Momentum: $\mathcal{P} + A_{xy,y} + 2B_{xy,y} + \beta u_{,yy} = 0$
- VCM constitutive equations + No flux of species and conformation at the wall
- Effect of microfluidics: $\delta_A = \dfrac{\lambda_A D_A}{H^2} \sim \dfrac{2\mathrm{sec} \cdot 10^{-9}\mathrm{m}^2/\mathrm{sec}}{(10^{-4})^2\mathrm{m}^2} = 2 \cdot 10^{-1}$

Helgeson and Vasquez et al., *J. Rheol.* (2009); Masselon et al., *PRE* (2010)

Pressure-Driven Channel Flow

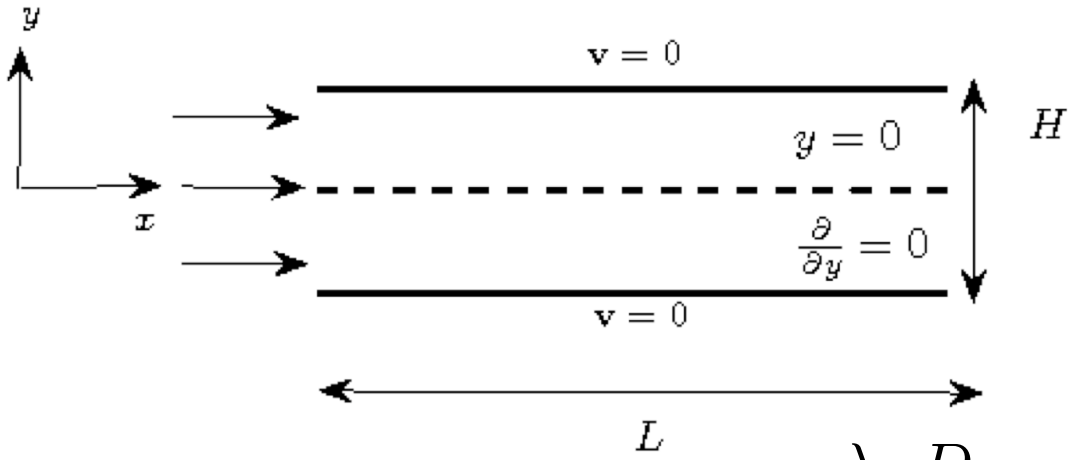

$$\mathcal{P} = \frac{\Delta p H}{L G_0} \qquad \delta = \frac{\lambda_A D_A}{H^2}$$

- The use of the boundary conditions of no flux of species and conformation at the wall requires the inclusion of a solvent viscosity:

$$\beta = \frac{\eta_s}{\eta_0} = 7 \times 10^{-5}$$

- Momentum: $\mathcal{P} + A_{xy,y} + 2B_{xy,y} + \beta u_{,yy} = 0$

- For slow flow dominated by the `A' species, the momentum balance becomes:

$$\mathcal{P} + A_{xy,y} - \beta\delta A_{xy,yyy} = 0$$

which results in a boundary layer at the wall of characteristic width $(\beta\delta)^{1/2}$.

Singular Perturbation

$$\mathcal{P} + A_{xy,y} - \beta\delta A_{xy,yyy} = 0$$

Outer $\quad \beta\delta \to 0$

$$A_{xy,y} = -\mathcal{P}$$

$$A_{xy} = -\mathcal{P}y$$

$$u_{,y} = A_{xy}$$

$$u = \frac{\mathcal{P}}{2}(0.25 - y^2)$$

Hagen-Poiseuille

Singular Perturbation

$$\mathcal{P} + A_{xy,y} - \beta\delta A_{xy,yyy} = 0$$

Outer $\quad \beta\delta \to 0$

$$A_{xy,y} = -\mathcal{P}$$

$$A_{xy} = -\mathcal{P}y$$

$$u_{,y} = A_{xy}$$

$$u = \frac{\mathcal{P}}{2}(0.25 - y^2)$$

Hagen-Poiseuille

Inner $\quad 0 < \beta\delta \ll 1$

$$A_{xy} = \mathcal{P}\left(-y + \sqrt{\beta\delta}\frac{\sinh\left(\sqrt{\frac{1}{\beta\delta}}y\right)}{\cosh\left(\frac{1}{2}\sqrt{\frac{1}{\beta\delta}}\right)}\right)$$

Expanding the solution ***near the wall*** and substituting into the inner equation for the velocity:

$$u_{,y} = A_{xy} - \delta A_{xy,yy}$$

$$u \simeq \frac{\mathcal{P}}{2}(0.25 - y^2) + \frac{\mathcal{P}\delta}{2}\left(1 - \exp\left\{\frac{1}{\sqrt{\beta\delta}}(y - 0.5)\right\}\right)$$

Wall Boundary Layer in Channel Flow

- The no flux boundary conditions, necessitated by the inclusion of diffusion, leads to boundary layer of characteristic width $(\beta\delta)^{1/2}$ which affects both shear stress and velocity, the latter of which presents as an apparent slip velocity:

$$u_s \simeq \frac{\mathcal{P}\delta}{2} = \frac{\Delta p' \lambda_A D_A}{G_0 L H}$$

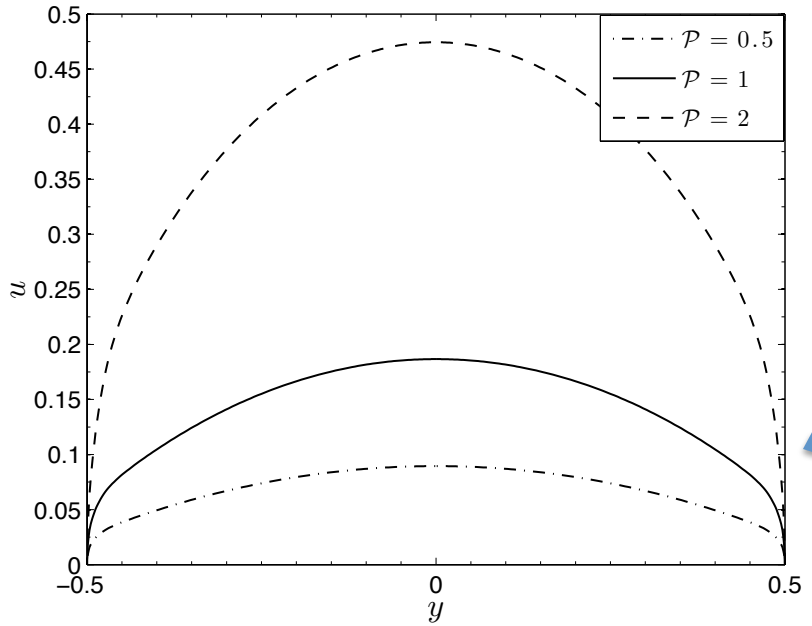

$$\frac{\mathcal{P}\delta}{2} = 0.1$$

$$\delta = \frac{\lambda_A D_A}{H^2} = 10^{-1}$$

Spurt & Hysteresis

- At the onset of shear banding there is sudden jump in the volumetric flow rate, `**spurt**'. For this value of the diffusivity, spurt occurs at $\mathcal{P} \simeq 2.39$.

The dimensional volumetric flow rate is given by:

$$\mathcal{Q}' = 2W \int_0^{H/2} u' dy'$$

When cast in dimensionless form, we have:

$$\mathcal{Q} = \frac{\lambda_{eff}}{H^2 W} \mathcal{Q}'$$

Flow rate of the Oldroyd-B model:

$$\mathcal{Q} \simeq \frac{1}{12} \mathcal{P}$$

Cromer et al., *JNNFM* (2010)

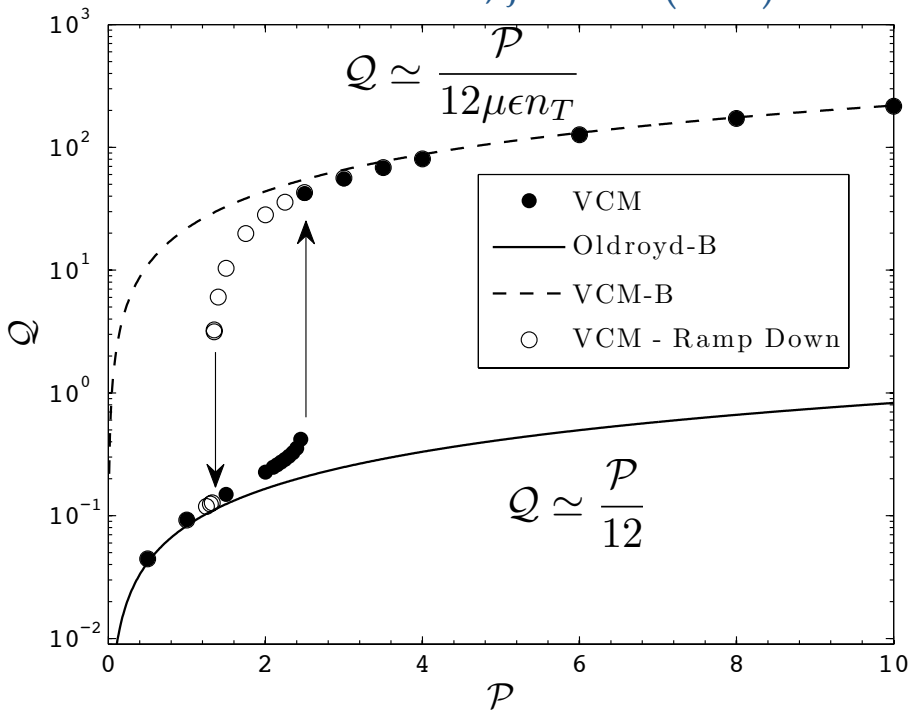

$$\mathcal{P} = \frac{\Delta p H}{L G_0} \qquad \delta = \frac{\lambda_A D_A}{H^2} = 10^{-3}$$

Spurt: Marín-Santibáñez et al., *JNNFM* (2009), de Vargas et al., *Rheo. Acta* (2003)

Shear Banded Velocity Profile in Channel Flow

Experiment vs. VCM

- Above a critical pressure drop, experiments of wormlike micelles exhibit shear banded velocity profiles with a low shear rate, plug-like flow in the center and a high shear rate region adjacent to the walls.

$H = 200\mu\text{m}$

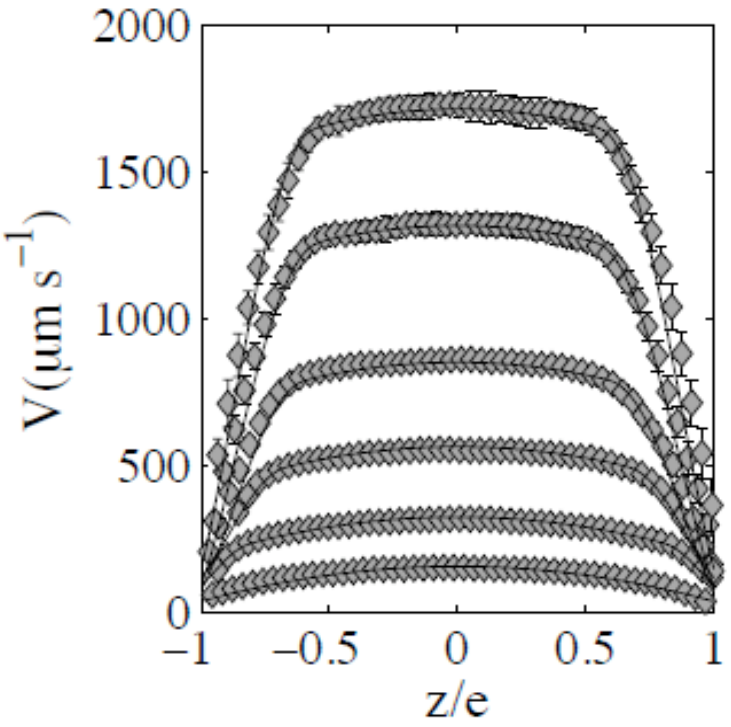

Experimental: Masselon et al., *PRE* (2010)
also: Masselon et al., *PRL* (2008), Nghe et al., *App.Phy.Let.* (2008), Callaghan et al., *J.Rheol.* (1997)

Shear Banded Velocity Profile in Channel Flow

Experiment vs. VCM

- Simulations show that, above a critical pressure gradient, the VCM model exhibits these shear banded velocity profiles.

$H = 200\mu\text{m}$

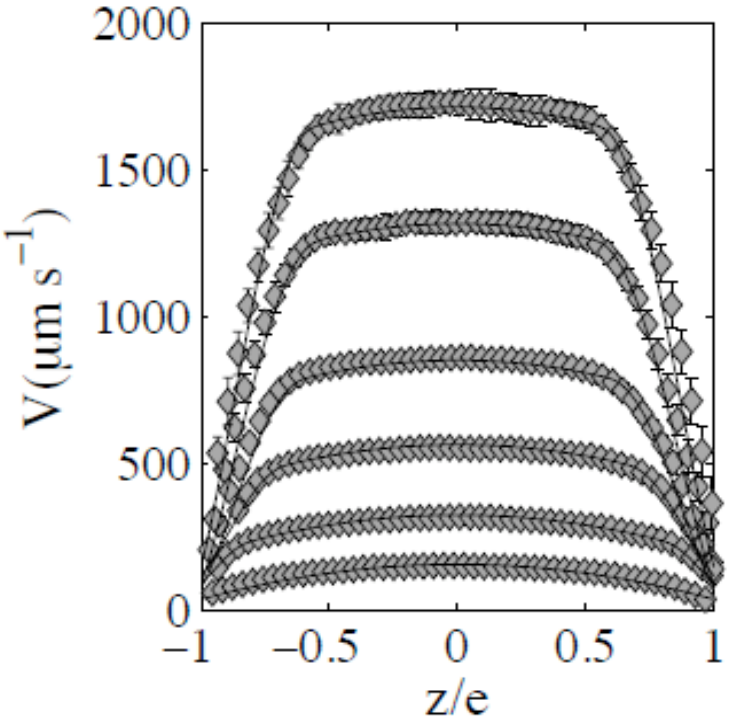

Experimental: Masselon et al., *PRE* (2010)
also: Masselon et al., *PRL* (2008), Nghe et al., *App.Phy.Let.* (2008), Callaghan et al., *J.Rheol.* (1997)

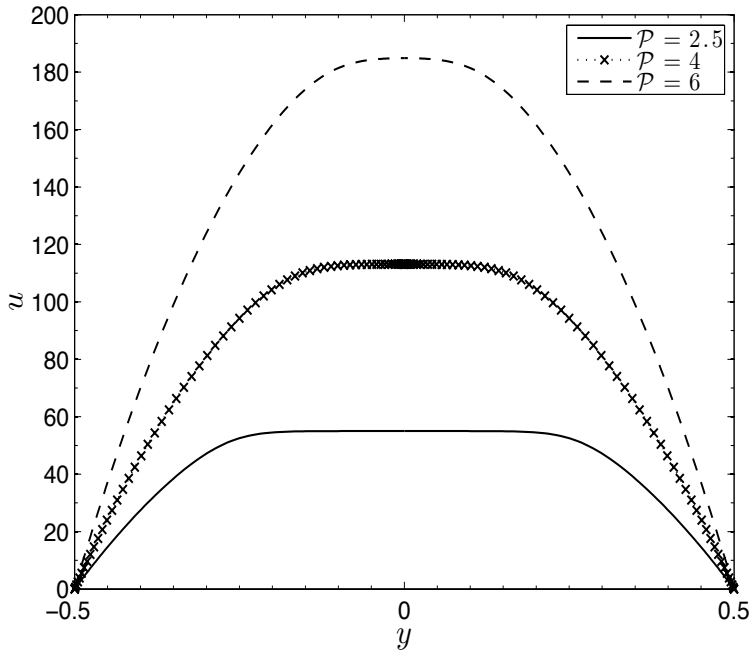

$$\mathcal{P} = \frac{\Delta p H}{L G_0} \qquad \delta = \frac{\lambda_A D_A}{H^2} = 10^{-1}$$

VCM

Shear Banded Velocity Profile in Channel Flow

Experiment vs. VCM

- For small diffusivity parameters the width of the kink $\ell = (\lambda_A D_A)^{1/2}$ joining the high and low shear bands becomes sharp and difficult to resolve numerically. Radulescu and Olmsted, *JNNFM* (2000)

$H = 200\mu\text{m}$

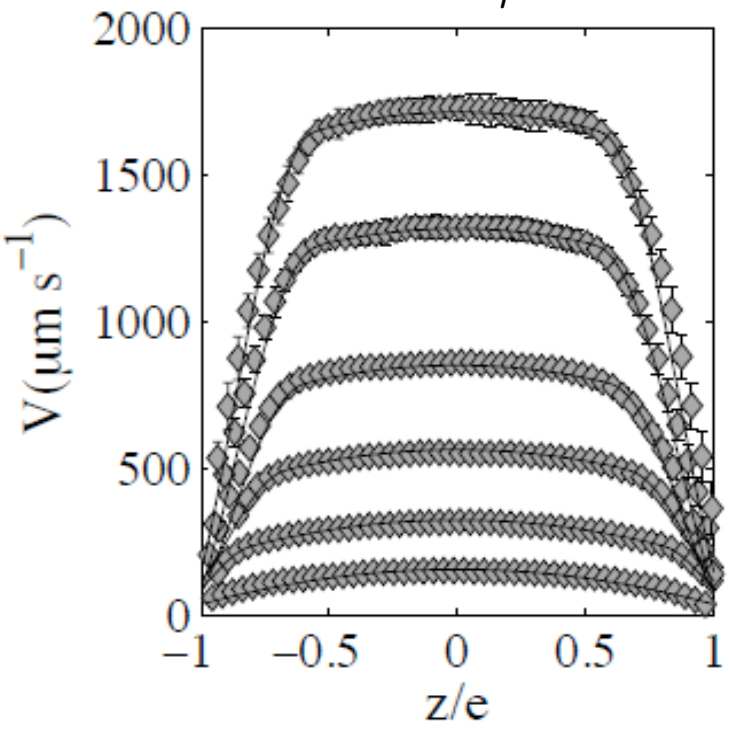

$\ell/H = \delta^{1/2}$

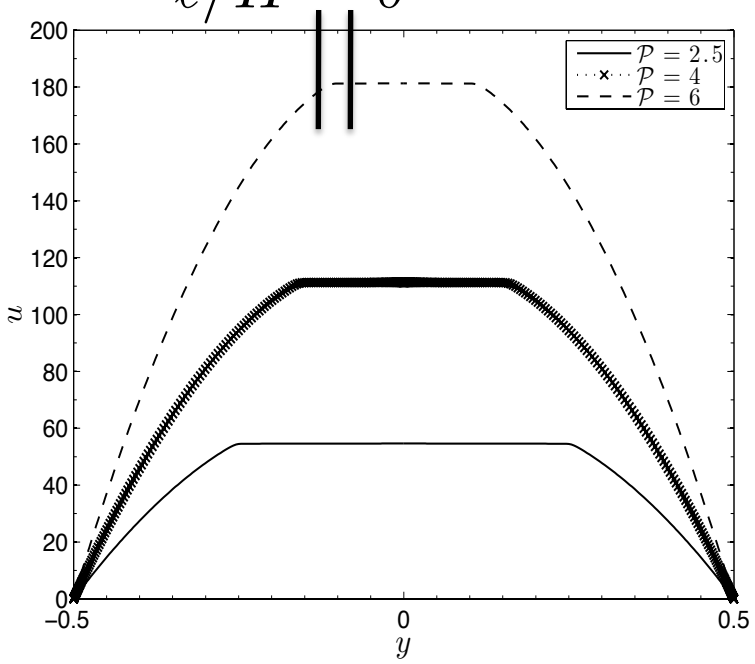

$$\mathcal{P} = \frac{\Delta p H}{L G_0} \qquad \delta = \frac{\lambda_A D_A}{H^2} = 10^{-3}$$

VCM

Experimental: Masselon et al., *PRE* (2010)
also: Masselon et al., *PRL* (2008), Nghe et al., *App.Phy.Let.* (2008), Callaghan et al., *J.Rheol.* (1997)

Effect of Diffusion on the Plateau - VCM

• Increased diffusion lowers the plateau (at lower shear rates), decreasing the stress at the interface between bands.

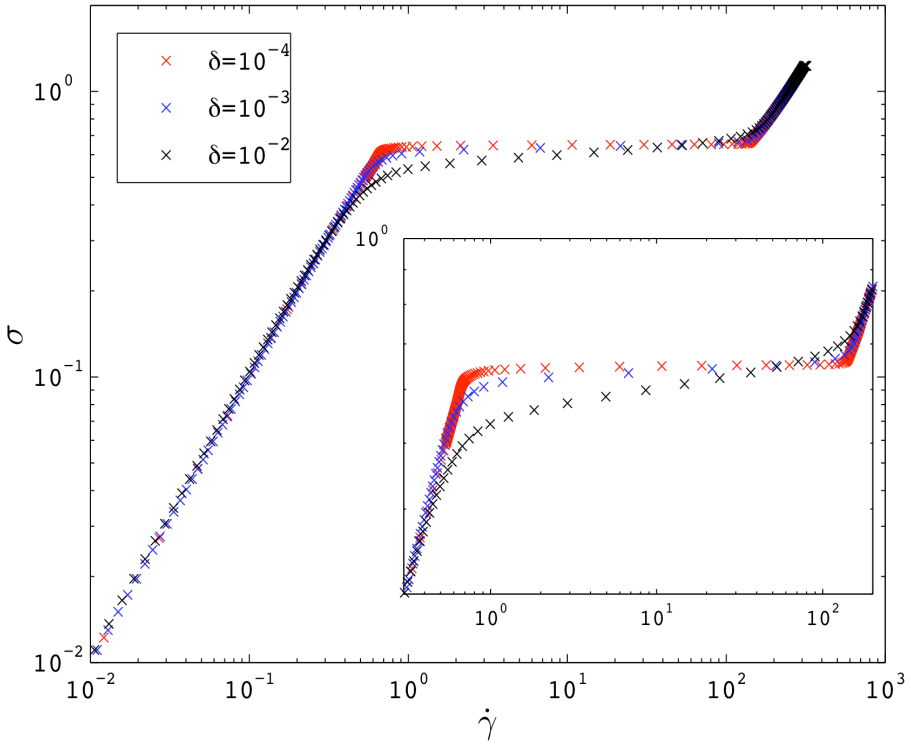

$$\mathcal{P} = \frac{\Delta p H}{L G_0} = 2.5$$

Experimental: Masselon et al., *PRE* (2010)

Flow Curve Collapse - VCM

• Increased diffusion lowers the plateau (at lower shear rates), decreasing the stress at the interface between bands.

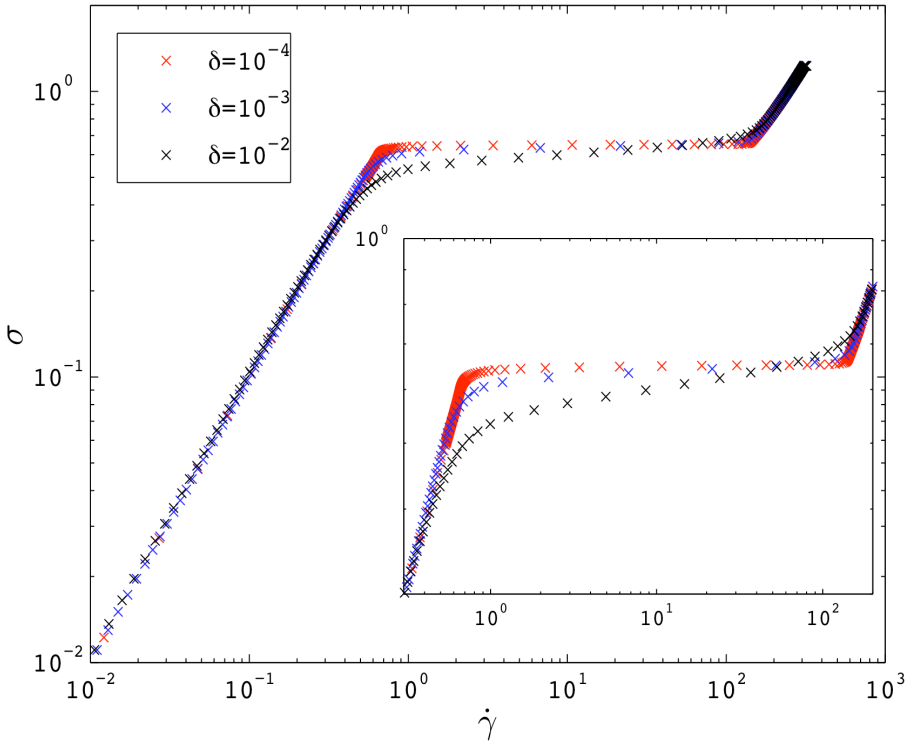

$$\mathcal{P} = \frac{\Delta p H}{L G_0} = 2.5$$

Experimental: Masselon et al., *PRE* (2010)

• Local flow curves collapse on top of each other when H is eliminated from dimensionless groups.

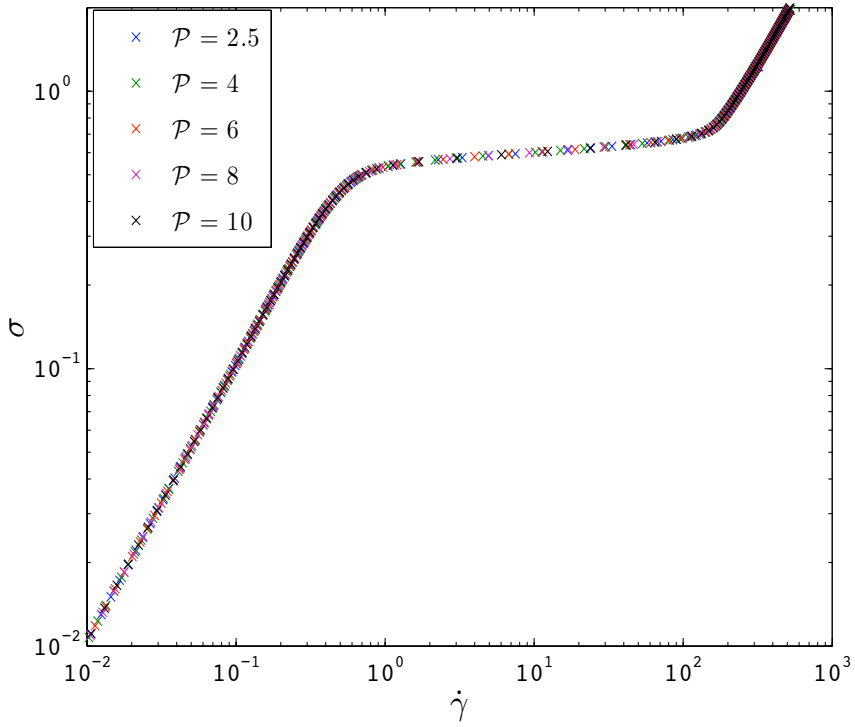

$$\mathcal{P}\delta^{1/2} = \frac{\sqrt{\lambda D}\Delta p}{L G_0} = 0.25$$

Cromer et al., *JNNFM* (In press)

Start-up of Plane Poiseuille Flow

1D Momentum + Constitutive Equations

Coupled, nonlinear system of time-dependent partial differential equations

The interfacial layer connecting the shear bands evolves in time on several different time scales:

- The layer forms at the wall and initially evolves on a fast, viscoelastic relaxation time scale.
- The layer then evolves on a slower diffusive time scale eventually settling into its steady position on a time scale proportional to $(\delta)^{-1/2}$.

  Radulescu et al., *Europhys. Lett.* (2003)

$$\mathcal{P} = \begin{cases} 0 & : t < 0 \\ \mathcal{P} & : t \geq 0 \end{cases}$$

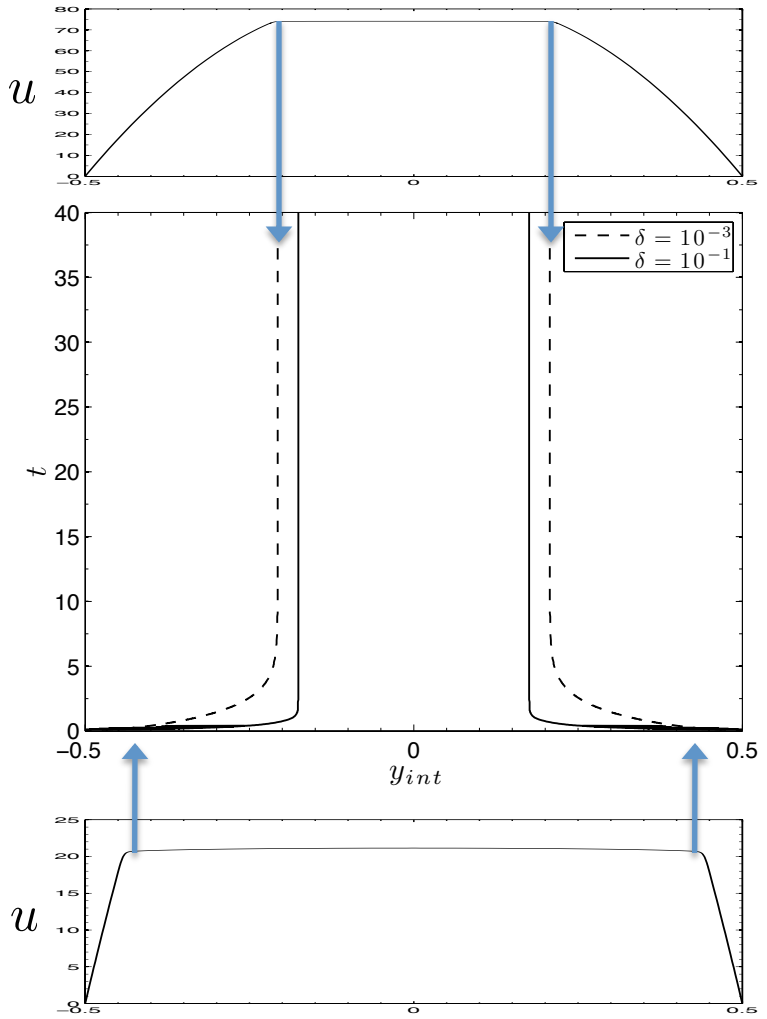

Flow Subdomains

1D Momentum + Constitutive Equations
Coupled, nonlinear system of time-dependent partial differential equations

The half-domain of shear banded flow can be separated into **4 subdomains**:

① The low shear rate, plug-like flow in the center of the channel.

② The interfacial layer connecting the shear bands, with characteristic width $\delta^{1/2}$.
Radulescu and Olmsted, *JNNFM* (2000)

③ The high shear rate flow closer to the solid wall.

④ The apparent slip boundary layer with characteristic width $(\beta\delta)^{1/2}$.

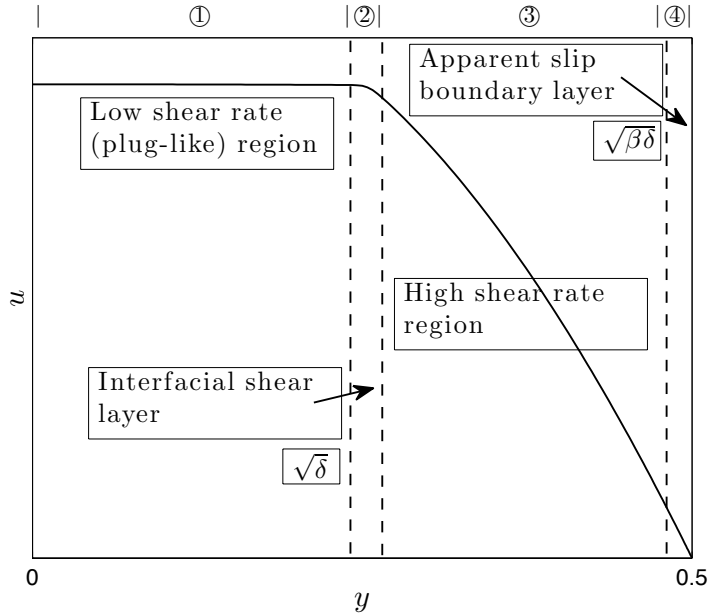

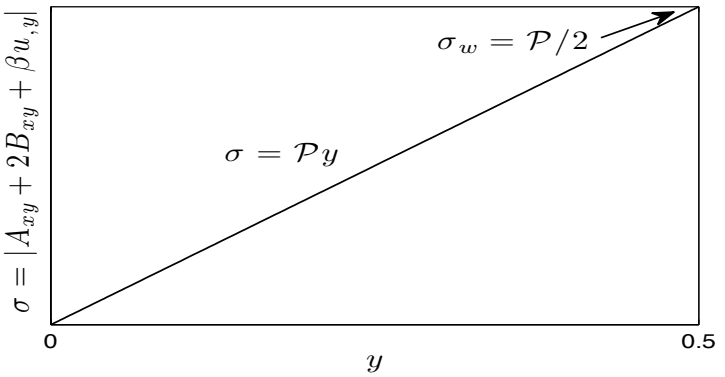

ADDS Method

1D Momentum + Constitutive Equations
Coupled, nonlinear system of time-dependent partial differential equations

- Adaptive Domain Decomposition Spectral (ADDS) Method:
  - Domain Decomposition
    - Patching Method
      - Orszag, *J. Comp. Phys.* (1980)
  - Interpolation
    - Barycentric Lagrange interpolation:
      - Berrut and Trefethen, *SIAM Review* (2004)

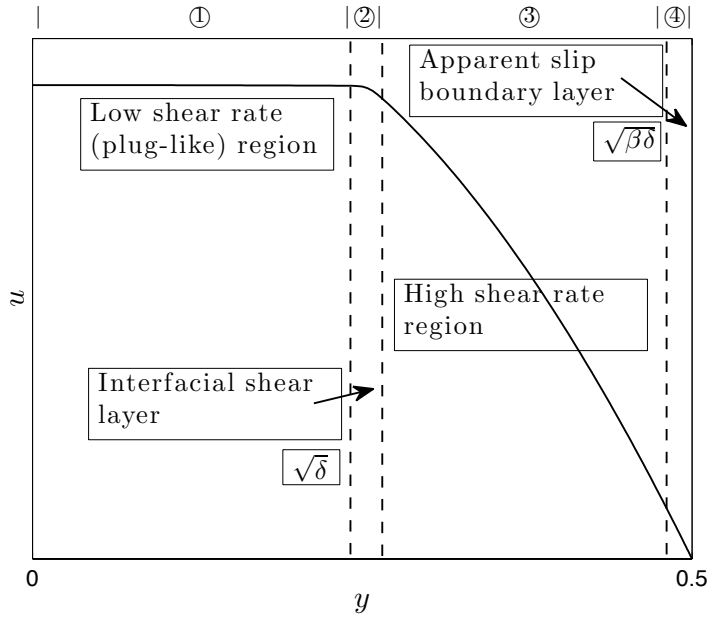

- 2nd order, variable step size, fixed leading coefficient BDF
  - Brenan, Campbell and Petzold, Numerical Solution of IVPs in DAEs, (© 1989)

Implementation of ADDS Method

- Using only a relatively small amount of collocation points , the ADDS method is able to resolve the time-dependent interior diffusive layer in a computationally efficient manner.

$$\mathcal{P} = \frac{\Delta p H}{G_0 L} = 4 \qquad \delta = \frac{\lambda_A D_A}{H^2} = 10^{-5}$$

Expected steady variation in shear stress

$$\sigma = A_{xy} + 2B_{xy} + \beta u_{,y}$$

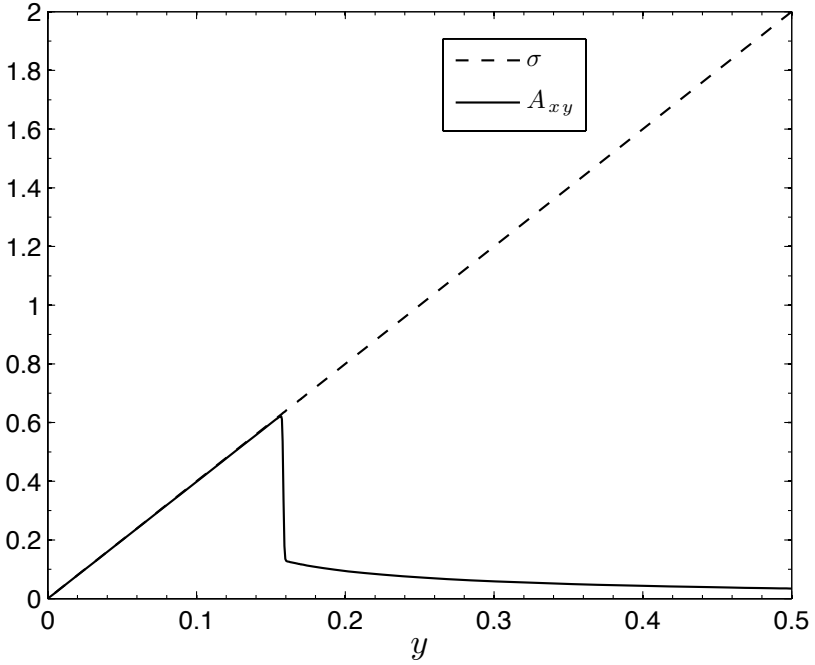

ADDS with 93 points

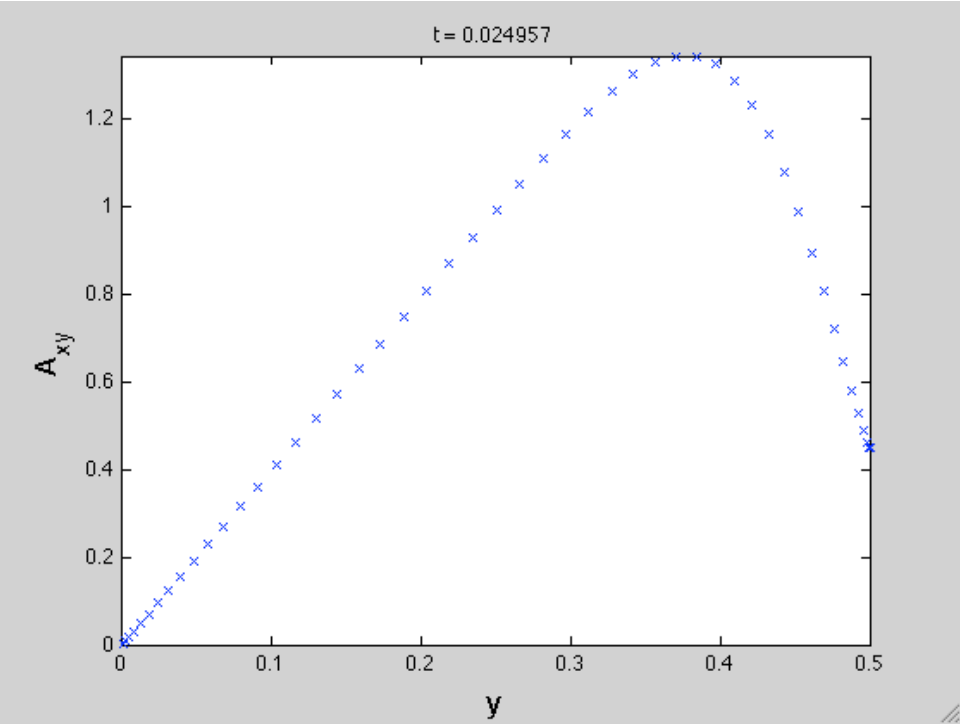

Channel Flow Instability

- Experiment:
  - Fluctuations *along the interface* between bands have been seen in the shear banded flow of wormlike micellar solutions in pipes and channels driven by a pressure gradient:
    - In the *flow direction*
      - Yamamoto et al., *Rheol. Acta* (2008)
    - In the *vorticity direction at the interface*
      - Nghe et al., *PRL* (2010)

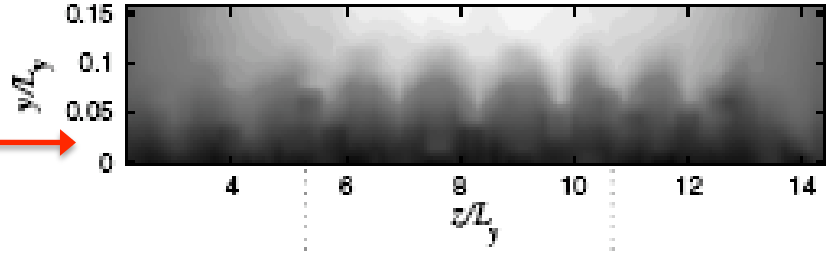

- Analytic:
  - Causes of instability
    - **First normal stress jump**
      - Wilson and Rallison, JNNFM (1999) – O-B
    - **Shear thinning**
      - Wilson and Rallison, JNNFM (1999) – W-M
    - **Shear banding**
      - Fielding and Wilson, JNNFM (2010) – J-S

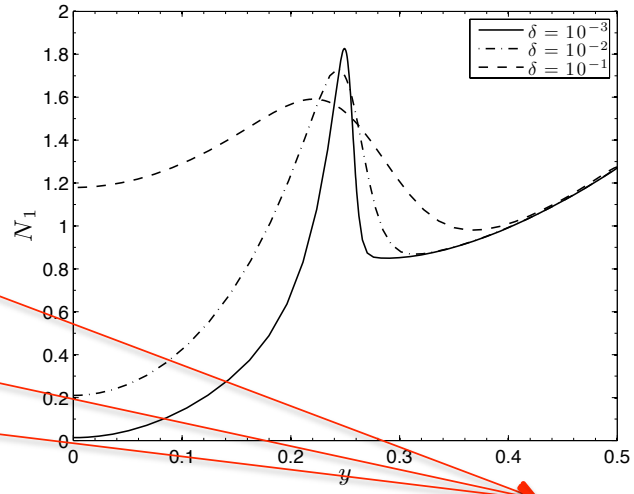

Cromer et al., *JNNFM* (to appear) - VCM

Linear Stability

The 1D base state is subjected to a perturbation of the form:

$$f = f^0(y) + \delta_s f^1(y) e^{i(kx-\omega t)}$$

$()^1$ is the eigenfunction which is a function of y only, k is the wavenumber in the flow direction, x, and $\omega = \omega_R + i\omega_I$ is the eigenvalue where $\omega_I > 0$ ➔ Blow up.

- The resulting system of equations form a generalized eigenvalue problem of the form:

$$\mathbf{Ax} = \omega \mathbf{Bx}$$

- **B** is singular due to the assumption of inertialess flow. This singularity produces infinite eigenvalues which complicates the solution of the eigenvalue problem.

- Thus, we adapt the method developed by Goussis and Pearlstein, *J. Comp. Phys.* (1989) to map the infinite eigenvalues onto the complex plane leaving the true eigenvalues of the system untouched.

VCM Unstable – Eigenfunctions

$\mathcal{P} = 2.5 \qquad \delta = 10^{-3} \qquad k = 2$

- Unstable eigenfunctions for the VCM model: Streamfunction. ψ and the velocity, u^1.
- The sharp gradients at the interface between the shear bands indicate local fluctuations of the interfacial layer.
- Superposition of base state and perturbation results in sinuous (odd; snake-like) flow.
- Similar to that seen for the Johnson-Segalman model. Fielding & Wilson *JNNFM* (2010)

ψ

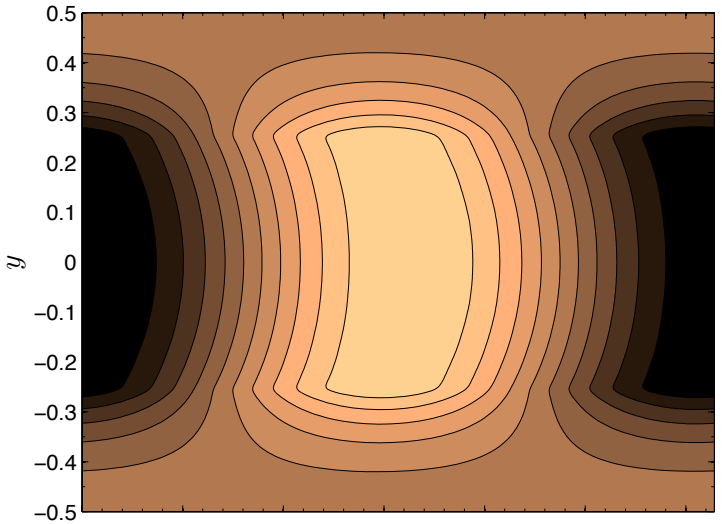

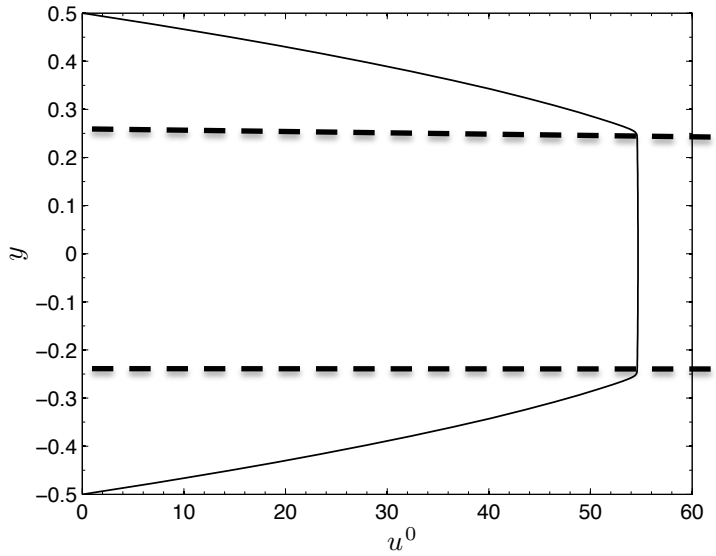

$$u^1 = \frac{\partial \psi}{\partial y}$$

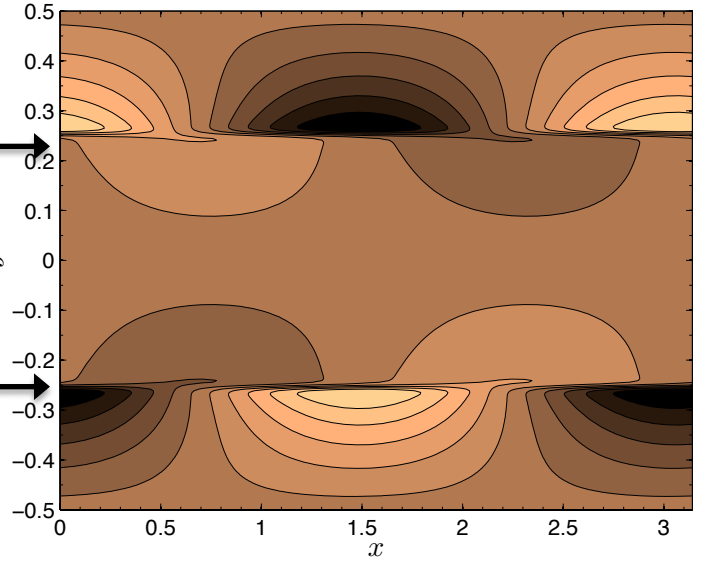

Role of Diffusion on Flow Stability

- The 1D, shear banded base state for the VCM model becomes linearly unstable to perturbations in the flow direction at the onset of shear banding, `spurt'.
  - ❖ For this value of the diffusivity, spurt occurs at $\mathcal{P} \simeq 2.39$.

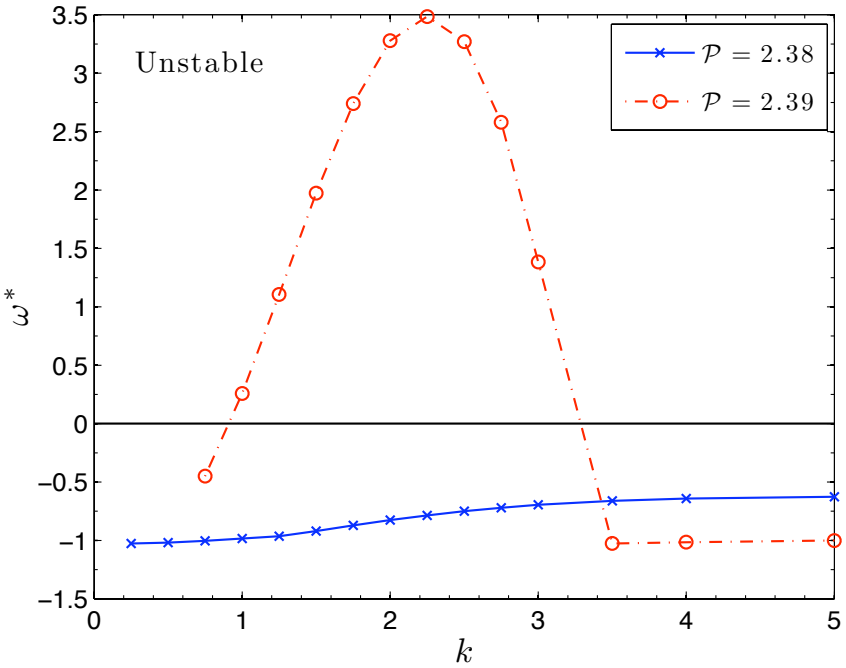

$$\delta = \frac{\lambda_A D_A}{H^2} = 10^{-3} \qquad \beta = 7 \times 10^{-5}$$

Role of Diffusion on Flow Stability

- The 1D, shear banded base state for the VCM model becomes linearly unstable to perturbations in the flow direction at the onset of shear banding, `spurt'.
  - ❖ For this value of the diffusivity, spurt occurs at $\mathcal{P} \simeq 2.39$.
  - ❖ As the value of the diffusivity is increased the flow becomes increasingly stable.

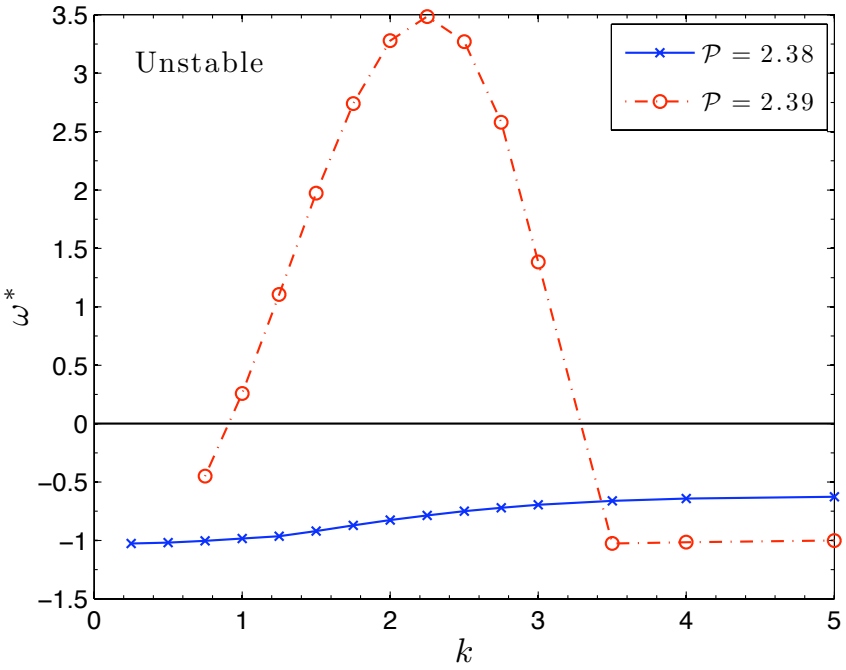

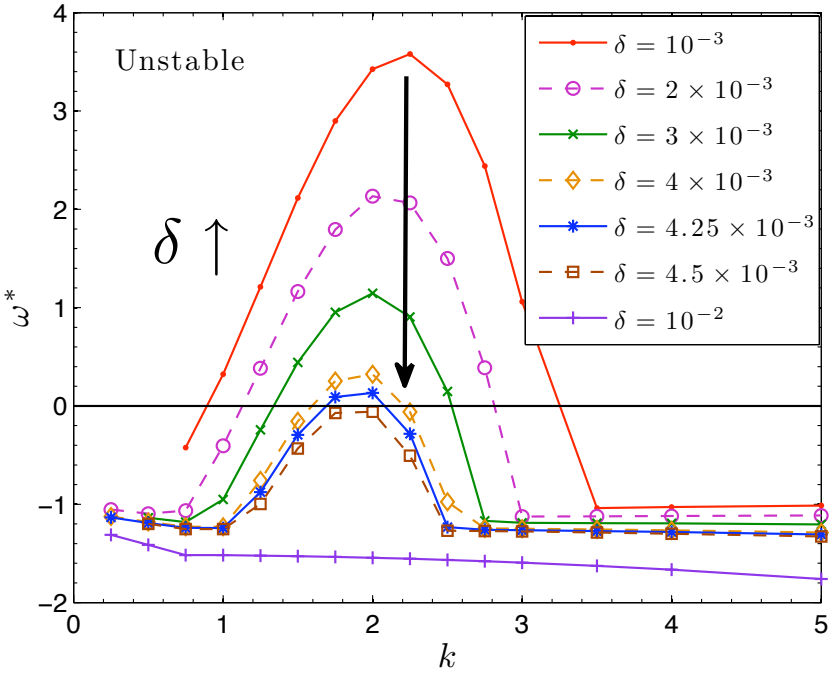

$$\delta = \frac{\lambda_A D_A}{H^2} = 10^{-3} \qquad \beta = 7 \times 10^{-5} \qquad \mathcal{P} = \frac{\Delta p H}{L G_0} = 2.5$$

Neutral Stability Envelope

- Neutral stability curves for the VCM model: $\omega^*(k;\mathcal{P},\delta)=0$
- Increased diffusivity, or decreased channel height, smoothes the kink in the velocity profile and progressively stabilizes the shear banded base flow.
- The critical diffusivity at which the flow of the VCM fluid becomes globally linearly stable is:

$$\delta_{crit} \simeq 4.51 \times 10^{-3}$$

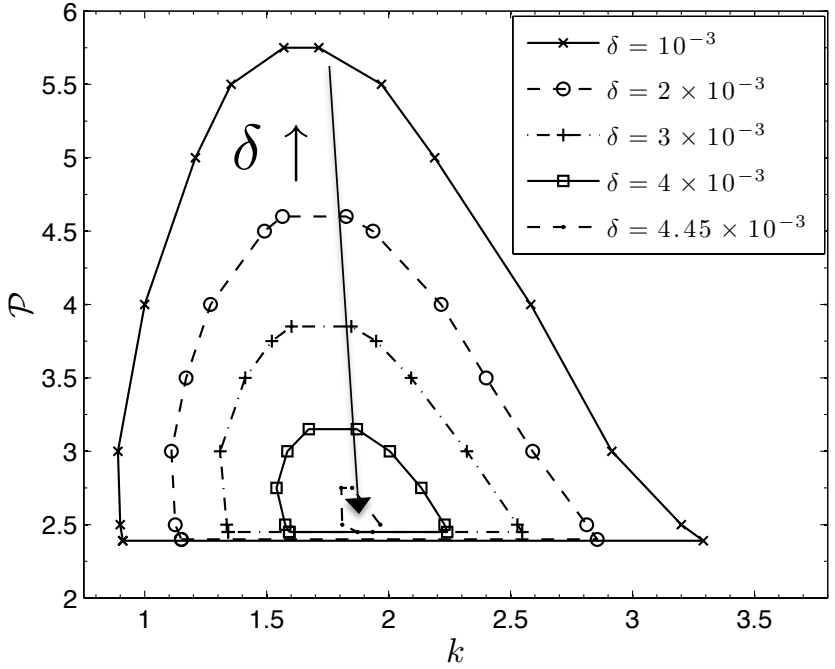

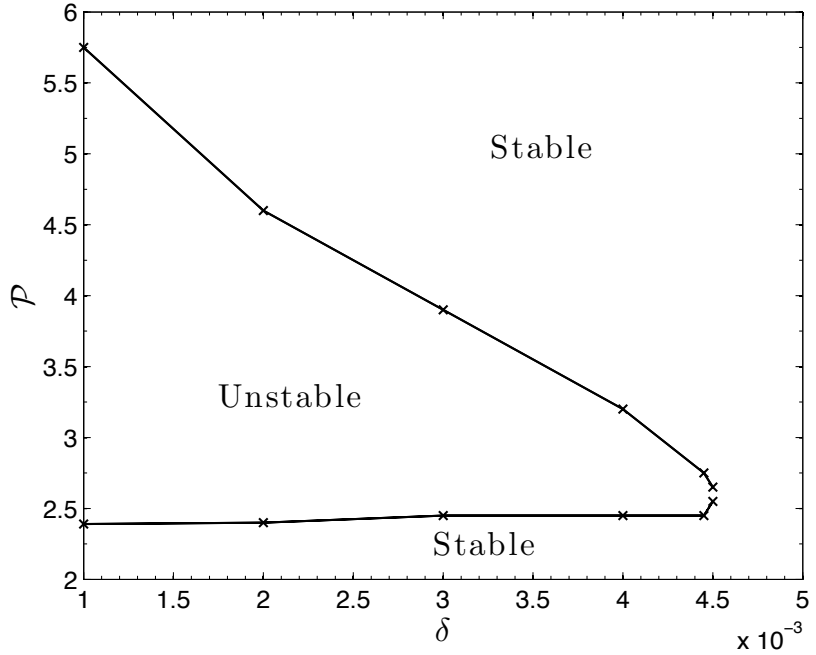

$$\mathcal{P} = \frac{\Delta p H}{L G_0} \qquad \delta = \frac{\lambda_A D_A}{H^2} \qquad \beta = 7 \times 10^{-5}$$

Transient Extensional Flow: FiSER

Bhardwaj, Miller, Rothstein, *J. Rheol.* (2007) 150/75 mM CPyCl/NaSal, *De*=2.6

Rupture for large extension rates (*De*), for smaller *De* failure through elastocapillary thinning. (transition between *De*=0.74 and 0.99)

"Dramatic rupture near axial midplane (at constant stress independent of *De*) likely stems from the local scission of individual wormlike micelle chains."

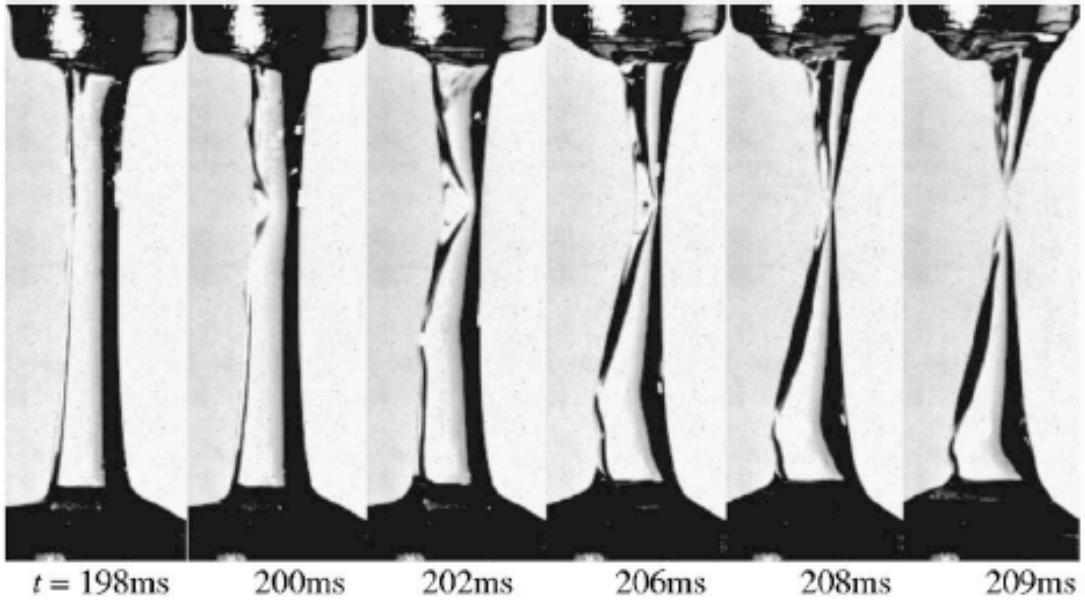

FIG. 6. Representative images of progressive filament rupture for the 150/75 mM CPyCl/NaSal solution at a *De*=2.6. The total duration of the failure event was determined to be 11 ms.

Governing Equations (VCM Model)

Number Densities:

$$n_\alpha(\mathbf{r},t) = \int \Psi_\alpha d\mathbf{Q}$$

$$\alpha = A,B$$

Configuration Tensors:

$$\mathbf{A} = \{\mathbf{QQ}\}_A = \int \mathbf{QQ}\Psi_A d\mathbf{Q}$$

$$\mathbf{B} = \{\mathbf{QQ}\}_B = \int \mathbf{QQ}\Psi_B d\mathbf{Q}$$

Constitutive equations

$$De_A \frac{Dn_A}{Dt} = \frac{1}{2} c_B n_B^2 - c_A n_A$$

$$De_A \frac{Dn_B}{Dt} = -c_B n_B^2 + 2c_A n_A$$

$$De_A \mathbf{A}_{(1)} + \mathbf{A} + n_A \mathbf{I} = c_B n_B \mathbf{B} - c_A \mathbf{A}$$

$$\epsilon De_A \mathbf{B}_{(1)} + B - \frac{n_B}{2} I = \epsilon \left[-2c_B n_B \mathbf{B} + 2c_A \mathbf{A} \right]$$

Hencky strain = $\varepsilon = \dot{\varepsilon}_0 t$

Deborah number = $De = \lambda_{eff} \dot{\varepsilon}_0 \qquad De_A = \lambda_A \dot{\varepsilon}_0$

Elastocapillary number = $Ec = G_0 R_0 / \sigma$

•Free Surface BC's at S := r – R(z,t) = 0

Kinematic Condition

$$\frac{DS}{Dt} = 0$$

Normal and Tangential Stress Balances

$$\mathbf{n} \cdot \mathbf{\Pi} \cdot \mathbf{n} = -2Ec^{-1}\kappa$$

$$\mathbf{t} \cdot \mathbf{\Pi} \cdot \mathbf{n} = 0$$

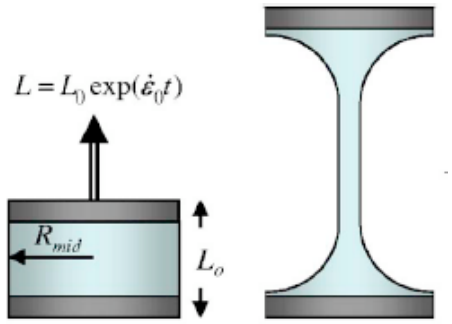

Homogeneous Uniaxial Extensional Flow

First Normal Stress Difference (Elastic Tensile Stress)

$$N_1 = A_{zz} - A_{rr} + 2(B_{zz} - B_{rr})$$

Extensional Viscosity

$$\eta_E = \frac{N_1}{De}$$

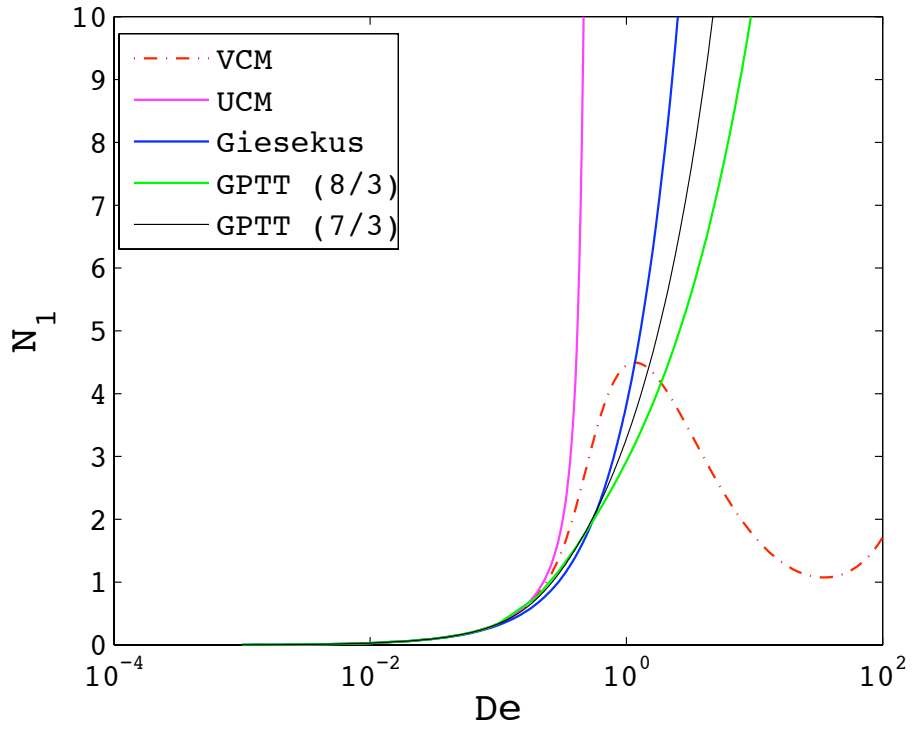

Steady tensile stress
Model comparison

Cromer et al, *Chem. Eng. Science* (2009)

1-D (Lagrangian) Inhomogeneous Transient Extension

X: Particle position in original reference frame

$z(X,t)$: Actual position of the particle

$$s = \frac{\partial z}{\partial X} \quad \text{Stretch;} \quad w_{,z} = \frac{s_{,t}}{s} \qquad R(X,t) = \frac{1}{\sqrt{s}}$$

$$\dot{\gamma} = \begin{pmatrix} -\frac{s_{,t}}{s} & 0 & 0 \\ 0 & -\frac{s_{,t}}{s} & 0 \\ 0 & 0 & 2\frac{s_{,t}}{s} \end{pmatrix}$$

Constitutive equations

Equation of motion:

$$3\beta De\frac{s_{,t}}{s^2} + \frac{N_1}{s} + \frac{Ec^{-1}}{\sqrt{s}} = f(t)$$

Total stretch constraint: FiSER

$$\int_0^1 s(X,t)dX = e^{\varepsilon}$$

Initial condition: $s(X,0) = 1 - \delta\cos(2\pi X)$

M. Renardy, *Rheol. Rev.* (1994)

VCM Filament Evolution

$\varepsilon = 0.1$

$De = 2, Ec^{-1} = 0$

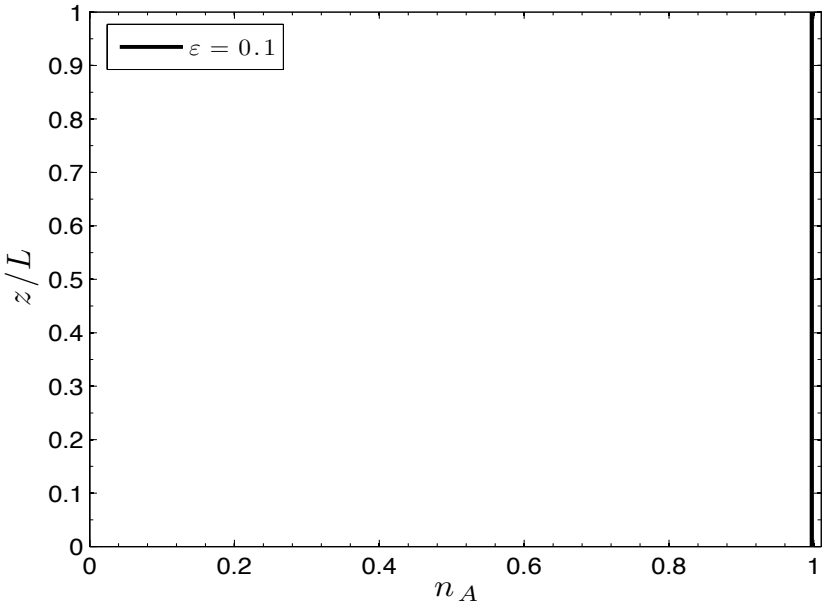

$n_B = n_T - 2n_A$

VCM Filament Evolution

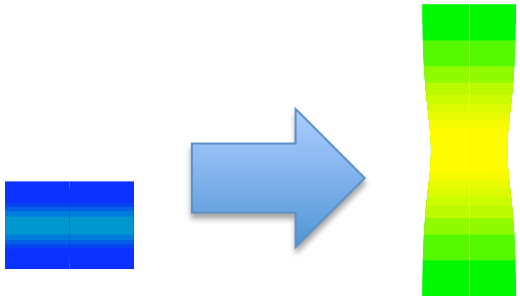

$\varepsilon = 0.1$ $\varepsilon = 1.2$

$$De = 2, Ec^{-1} = 0$$

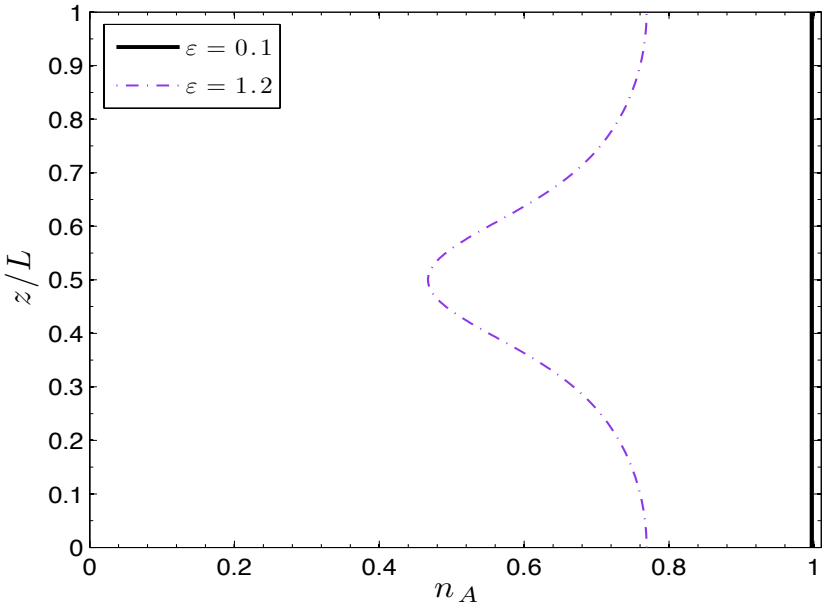

$$n_B = n_T - 2n_A$$

VCM Filament Evolution

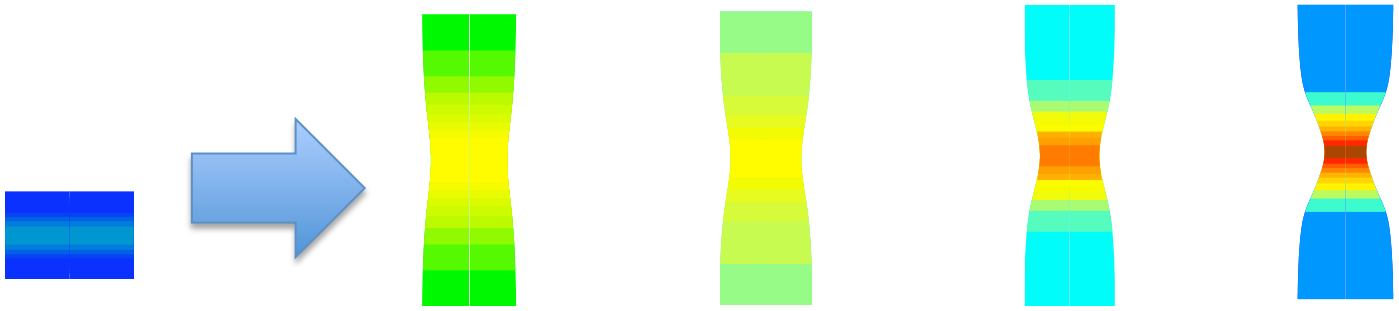

$\varepsilon = 0.1$ $\varepsilon = 1.2$ $\varepsilon = 1.215$ $\varepsilon = 1.23$ $\varepsilon = 1.24$

$De = 2, Ec^{-1} = 0$

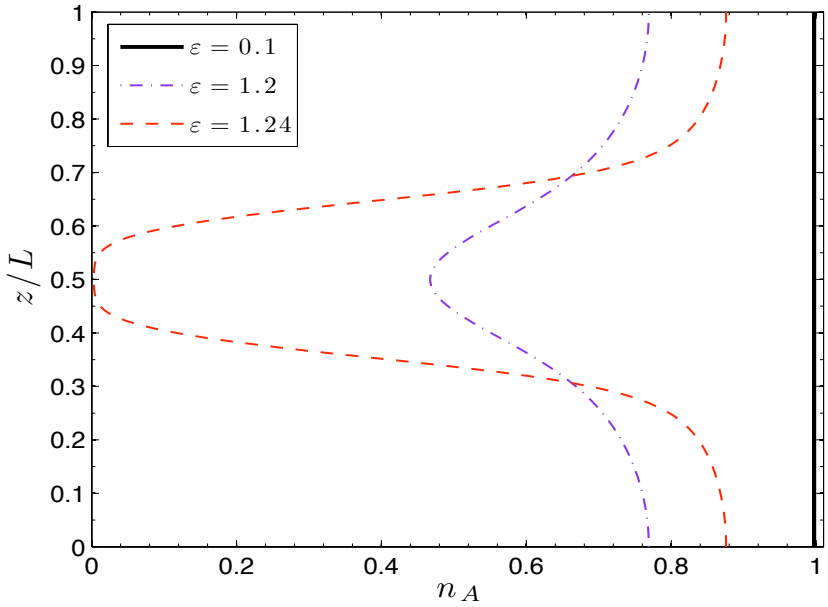

$n_B = n_T - 2n_A$

VCM Filament Evolution

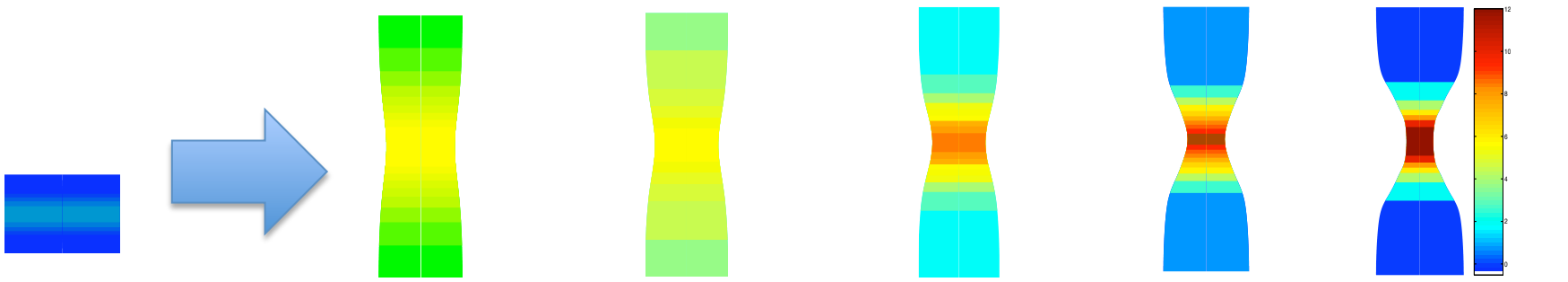

$\varepsilon = 0.1$ $\varepsilon = 1.2$ $\varepsilon = 1.215$ $\varepsilon = 1.23$ $\varepsilon = 1.24$ $\varepsilon = 1.2433$

$$De = 2, Ec^{-1} = 0$$

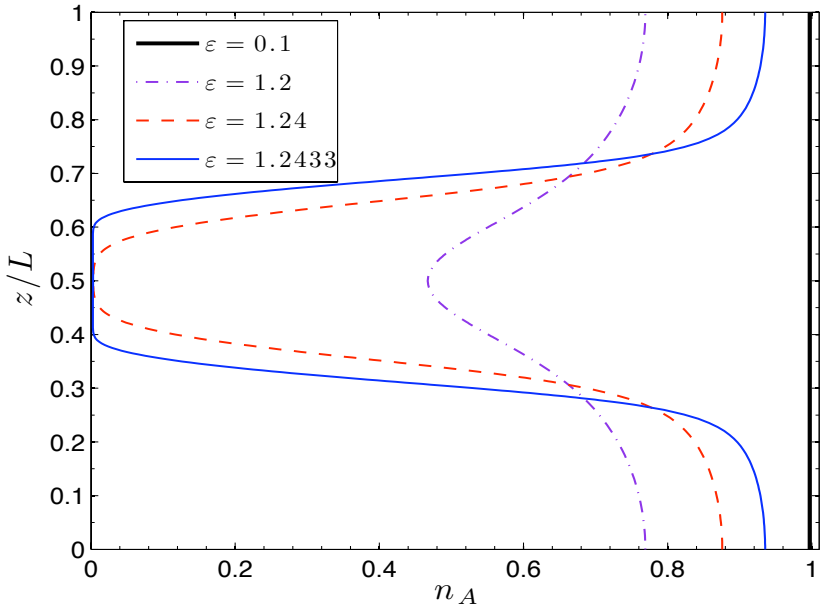

$$n_B = n_T - 2n_A$$

VCM Filament Evolution

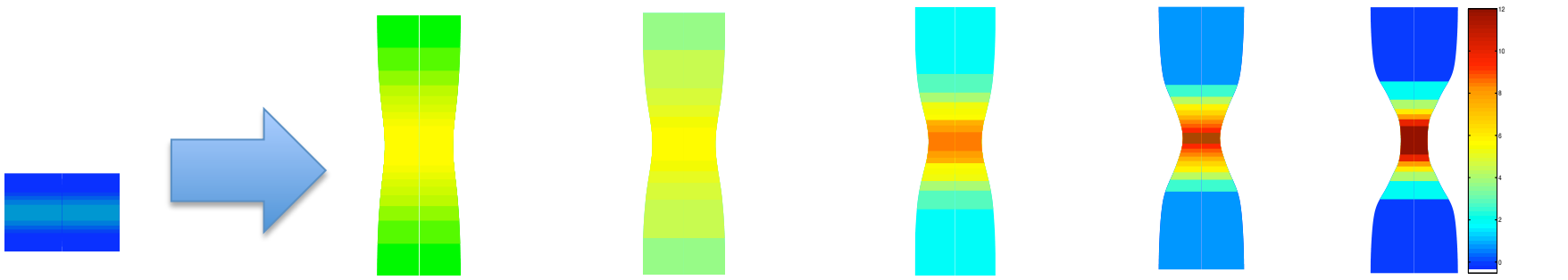

$\varepsilon = 0.1$ $\varepsilon = 1.2$ $\varepsilon = 1.215$ $\varepsilon = 1.23$ $\varepsilon = 1.24$ $\varepsilon = 1.2433$

$$De = 2, Ec^{-1} = 0$$

"This filament failure likely stems from the scission of wormlike micelles resulting in a dramatic breakdown of the micelle network *en masse*." Rothstein, *J. Rheol.* (2003)

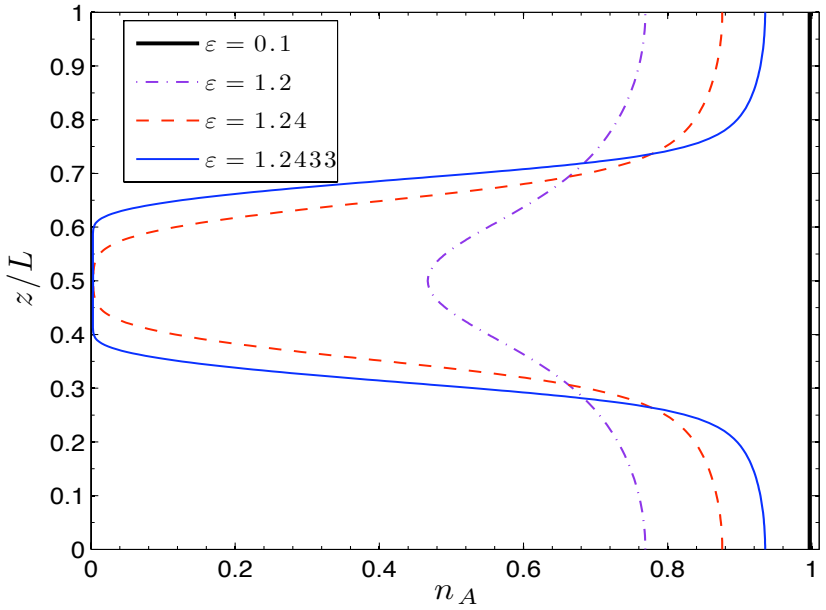

$$n_B = n_T - 2n_A$$

VCM vs. Experiment -- Rupture

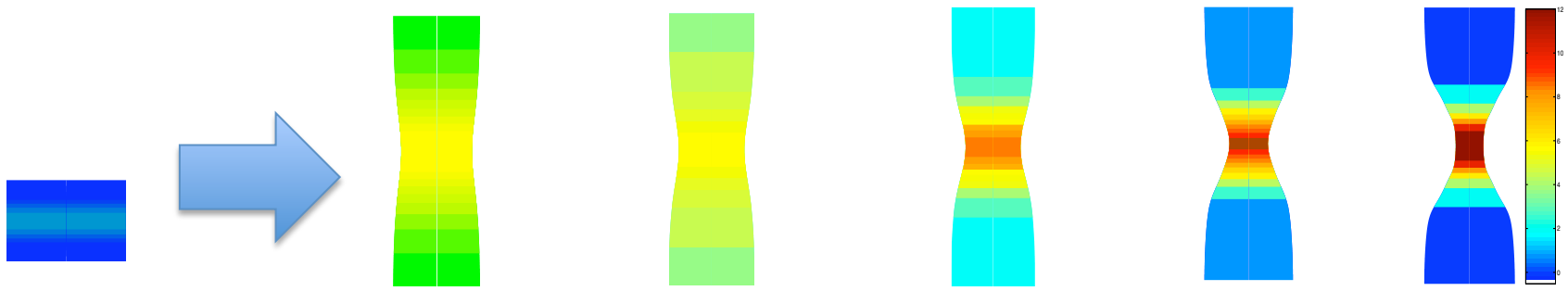

$\varepsilon = 0.1$ $\varepsilon = 1.2$ $\varepsilon = 1.215$ $\varepsilon = 1.23$ $\varepsilon = 1.24$ $\varepsilon = 1.2433$

$\Delta t \approx 4.7\text{ms}$ $\Delta t \approx 4.7\text{ms}$ $\Delta t \approx 3.15\text{ms}$ $\Delta t \approx 1\text{ms}$

$$De = 2, Ec^{-1} = 0$$

Strong recoil at the end plates (accompanied by dramatic thinning at the axial mid-plane)

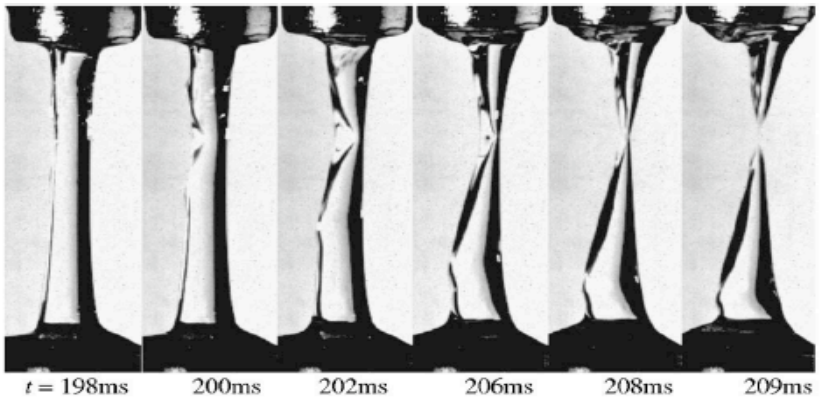

FIG. 6. Representative images of progressive filament rupture for the 150/75 mM CPyCl/NaSal solution at a *De*=2.6. The total duration of the failure event was determined to be 11 ms.

Bhardwaj et al., *J. Rheol.* (2007)

Recap/Conclusions

- VCM Model
  - Framework for consistently developing nonlocal constitutive models that couple evolutions in stress, number density and diffusivity.
- Planar channel flow – VCM
  - Boundary layer resulting from the inclusion of solvent viscosity and diffusion. Time-dependent interior (shear) layer of characteristic width $\sqrt{\delta}$.
  - ADDS method uses a domain decomposition Chebyshev collocation patching method to resolve the layers and barycentric Lagrange interpolation to adapt domains in time.
- Linear Stability – VCM channel flow
  - The 1D banded channel flow becomes linearly unstable at the onset of shear banding creating sinuous disturbances along the channel. Increasing the dimensionless diffusivity, or decreasing the channel height, progressively stabilizes the flow: $\delta_{crit} \geq 4 \times 10^{-3}$.
- Extensional flow – VCM
  - A VCM filament can undergo a dramatic rupturing event, similar to experiment, that is accompanied by the long chains breaking *en masse*.